OPTIMIZATION OF A TWO STAGE LIGHT-GAS GUN

TEES-9075-CR-72-02

by

RICHARD J. RYNEARSON and JAMES L. RAND

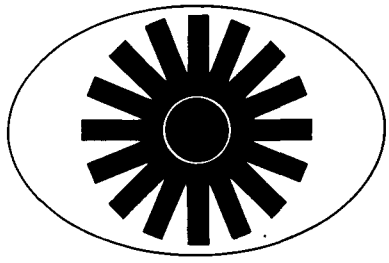

TEES

TEXAS ENGINEERING EXPERIMENT STATION
TEXAS A&M UNIVERSITY
COLLEGE STATION TEXAS 77843

August 1972

Prepared for

NASA Manned Spacecraft Center

Meteoroid Sciences

Houston, Texas 77058

Under Contract NGR 44-001-106

OPTIMIZATION OF A TWO STAGE LIGHT-GAS GUN

TEES-9075-CR-72-02

by

Richard J. Rynearson and James L. Rand

September 1972

Prepared for
NASA Manned Spacecraft Center
Meteoroid Sciences
Houston, Texas 77058
Under NASA Grant NGR 44-001-106

Prepared by
Texas Engineering Experiment Station
Texas A&M University
College Station, Texas 77843

FOREWORD

This report, TEES 9075-CR-72-02, is submitted by the Texas Engineering Experiment Station in partial fulfillment of NASA Grant NGR 44-001-106. It has also been submitted by Richard J. Rynearson to the Graduate College of Texas A&M University in partial fulfillment of the requirements for the degree of Master of Science in Aerospace Engineering in December 1972.

This task is part of a continuing effort to assist and enhance the engineering activities of the National Aeronautics and Space Administration - Manned Spacecraft Center.

ABSTRACT

This report deals with the performance characteristics of the Texas A&M University light-gas gun. A review of basic gun theory and popular prediction methods is presented. A computer routine based on the simple isentropic compression method is presented and discussed. Results from over 60 test shots are given which demonstrate an increase in gun muzzle velocity from 9,100 ft/sec. to 19,000 ft/sec. The data gathered indicated the Texas A&M light-gas gun more closely resembles an "isentropic compression" gun rather than a "shock compression" gun. Suggestions for future work conclude the report.

ACKNOWLEDGEMENT

The authors wish to express their appreciation to Mr. Burton G. Cour-Palais and Mr. Thomas D. Thompson of the Manned Spacecraft Center for their advice and assistance in making this gun operational. In addition the authors are indebted to Mr. Otto K. Heiney for providing the program used to compute gun performance. The authors are indebted to Mr. James Hanna for his work on the instrumentation system. The Space Technology Division and Mechanics and Materials Research Center of Texas A&M University gave significant support to the development of this gun. The miniature meteorite range and financial support were obtained under the National Aeronautics and Space Administration Grant, NGR 44-001-106.

TABLE OF CONTENTS

LIST OF TABLES

LIST OF FIGURES

NOMENCLATURE

Variable	
a	= speed of sound
A	= cross sectional area
E	= energy term
g	= acceleration of gravity
L	= barrel or pump tube length
M	= projectile mass or gas mass
M.W.	= gas molecular weight
N_B	= mass of gas released by burning propellant
p	= average chamber pressure
$\bar{p}$	= average projectile base pressure
R	= real gas constant
$\bar{R}$	= universal gas constant
r	= burning rate
S_B	= burning area
T	= average temperature
u	= projectile or gas velocity
U	= piston velocity
V	= chamber volume
V'	= reduced volume
ΔX	= reference distance
δ	= propellant gas energy factor
η	= covolume

γ = specific heat ratio

ρ = gas density

ρ_p = propellant density

Subscripts

b = projectile base

f = final condition

m = muzzle condition

o = initial condition

r = reservoir

t = time plane

Δt = time increment

CHAPTER I

INTRODUCTION

Since 1945 there has been a considerable amount of research concerned with techniques for launching projectiles to high velocities. In the first few years following World War II the military conducted the bulk of this research in the hopes of being able to simulate the hypervelocity flight of various ballistic missle systems. Interest in high speed guns was again stimulated in the 1950's with the emergence of the U. S. space program and in particular concern for the possible hazards of meteoroid impact during space missions.

The gun emerged as the primary tool in this research. Typical muzzle velocities at the beginning of this period were around 10,000 ft/sec. As a basic understanding of the internal ballistics of guns was obtained the muzzle velocity over a short number of years was dramatically increased to over 37,000 ft/sec. The highest muzzle velocities were obtained using special types of guns whose characteristics took advantage of the subtleties of internal ballistic theory. Of these the two stage light-gas gun became the most widely used.

The two stage light-gas gun utilizes a conventional gas propelled piston to compress a low molecular weight gas, usually

---

The citations on the following pages follow the style of the AIAA Journal.

hydrogen, to a high temperature and pressure in a pump tube. At a specified pressure a break valve opens allowing the projectile to accelerate down the launch tube. Figures (1) and (2) illustrate the components of the gun and the steps in a typical launch cycle. Many factors influence gun performance but these may be grouped into two main categories. First are those dealing with gun geometry. Pump tube diameter, powder chamber volume, and launch tube length are all examples of parameters which specify the gun geometry. The second category could be called loading conditions. Powder charge, piston mass, and initial gas pressure are good examples. In designing a new gun or analyzing an existing one these factors must be taken into account.

During the past year Texas A&M University has installed a small scale two stage light-gas gun at the TEES Hypervelocity Laboratory. The gun was obtained from the Manned Spacecraft Center in Houston, Texas where it was used for meteoroid impact studies. Unfortunately very little documentation or performance data accompanied the gun components to Texas A&M. A need arose to establish the performance characteristics of the gun and to document the entire gun system. Since the gun's geometry was basically fixed, the loading conditions became of primary concern in regard to performance.

This paper deals with the performance characteristics of Texas A&M's light-gas gun facility. A review of the literature concerning light-gas guns and their development is given first. Due to the volume of work conducted in this area this survey is limited to

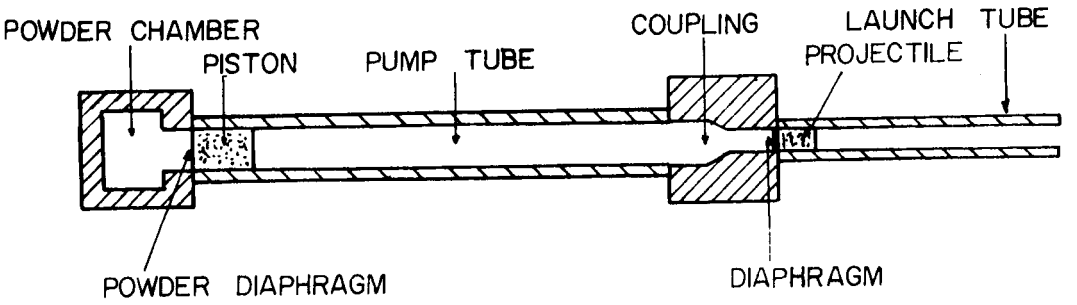

Figure 1 Schematic of Light Gas Gun

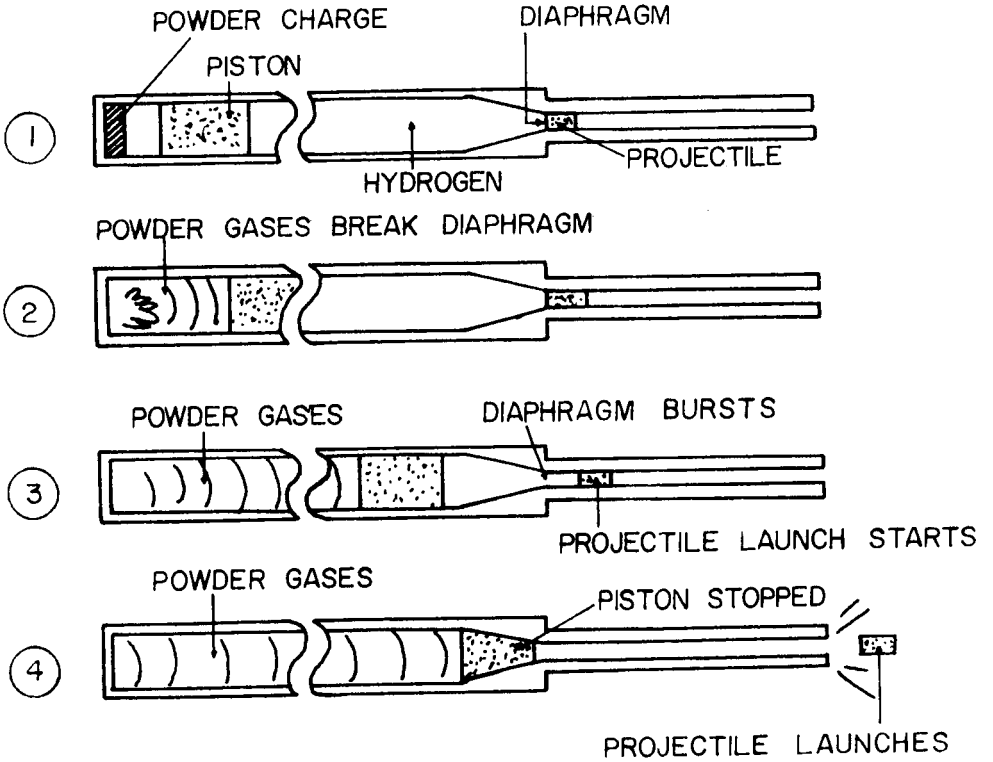

Figure 2 Gun Launch Cycle

information which was readily available and pertinent to the performance study. A discussion of the important theoretical concepts for light-gas guns is included as presented in the literature. The main emphasis here is to point out those facts which directly influence the choice of loading parameters rather than a complete theoretical development for light-gas guns which can be found in Siegel[1] or a number of references. A discussion of previous parametric studies concludes the literature survey. An explanation of the theoretical basis of the computer code used in this study is presented along with its limitations. The experimental program is described next with a description of the equipment used and results from over 60 test firings. The final portion of the thesis attempts to reconcile experimental observation with theoretical predictions and recommendations for future work are made.

CHAPTER II

LITERATURE SURVEY

2.1 Early Development

The first light-gas gun was developed by Crozier and Hume in 1946 at the New Mexico School of Mines[2]. Hydrogen was compressed by a single stroke piston driven by a gunpowder propellant. At that time it was felt that the compression ratio required by a piston-driven gun would make the pump tube impractically large for a barrel diameter greater than 20 mm. For this reason a number of years passed before further light-gas gun development was attempted. During this time various other techniques were explored to heat and compress the driver gas. Among these were various improved combustion processes which utilized stoichiometric mixtures of oxygen and hydrogen burned in an inert helium driver gas. Also various electric discharge techniques were developed. Somewhat later, Glass[3] authored a report which summarizes various driver techniques including the piston-compression process.

Light-gas gun work was revived in 1955 by Charters[4] at the NASA-Ames Research Center. A small light-gas gun utilizing piston-compressed hydrogen was built. Theoretical calculations had shown that a high speed gun of practical dimensions and capable of launching aerodynamic models at velocities in excess of 20,000 ft/sec, could be developed. During this research, Charters also developed a simple

way to analyze the gun cycle. This particular method and others will be discussed later. Concurrent with the work at Ames, a second type of light-gas gun was developed at the U. S. Naval Ordnance Laboratory under the direction of Z. I. Slawsky. The results of these early gun studies showed the light-gas gun to be a practical technique for launching high speed aerodynamic models. As a result, various laboratories in the United States, Canada, and England began improving light-gas gun technology. The light-gas gun has since become an invaluable tool to generate flight speeds up to 11 Km/sec.[2]

2.2 Basic Gun Theory

Various references[1,2,3] give a complete development of the internal ballistics of high speed guns, but a brief outline of the more important points will be given here. The easiest way to get a feel for those factors which influence projectile velocity is to consider a simple gun model. Figure 3 gives the analysis offerred by Siegel.[1] The following expression indicates the essential factors upon which projectile velocity depends:

$$U_{proj} = \sqrt{2\ \bar{p}\ AL/M} \qquad (1)$$

where $\bar{p}$ is the average projectile base pressure. In order to increase projectile velocity, the terms under the square root must be changed accordingly. Within the limitations of a fixed gun geometry the quantities $\bar{p}$ and M are the only terms which are not specified. Assuming a particular projectile mass is chosen, $\bar{p}$ becomes the sole

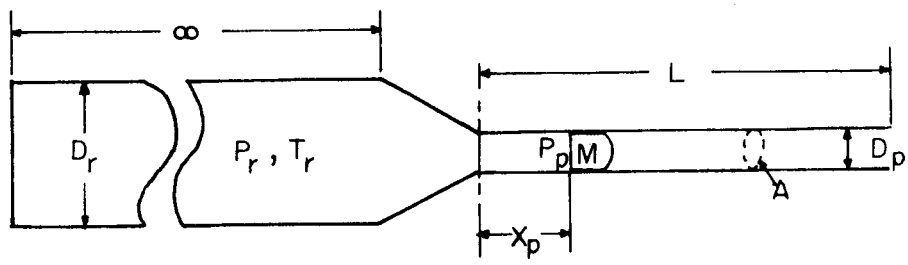

NEWTON'S LAW,

$$F_p = P_p A = \frac{d(MU_p)}{dt}$$

$$P_p = M \frac{d(U_p^2/2)}{dX_p} \qquad (1)$$

Integrating, (1),

$$\frac{Mu^2}{2} = A \int_0^L P_p \, dX_p \qquad (2)$$

where, u = Projectile Muzzle Velocity

Introduce $\bar{p}$, the Spatial Average Propelling Pressure defined as,

$$\bar{p} \equiv \frac{1}{L} \int_0^L P_p \, dX_p \qquad (3)$$

Substituting (3) into (2) yields,

$$u = \sqrt{2 \bar{p} \frac{AL}{M}} \qquad (4)$$

Figure 3: Simple Gun Model with Sample Calculation

quantity controlling the projectile velocity. Any efforts to increase gun velocity is then a search for a method to maximize $\bar{p}$.

It can be shown that $\bar{p}$ is maximized by producing a constant base pressure on the projectile.[1] From a practical point of view this is very difficult to obtain. By analyzing a simple launcher consisting of a reservoir and launch tube of the same diameter, and by assuming the expansion is nonsteady, one-dimensional, isentropic flow, the following important relationship can be obtained[2]:

$$dp = -\rho a\, du \tag{2}$$

which states the change of pressure with velocity is dependent upon ρa, termed the "acoustic impedance" of the propellant gas. In order to obtain a high increment in velocity requires a low acoustic impedance. This basically controls the selection of the propellant gas. It should also be mentioned that, except in the unrealistic case in which ρa is zero, an increase in projectile velocity neccesitates a corresponding decrease in base pressure.

An expression for the acoustic impedance in terms of the reservoir conditions can be obtained from the following relations[2]:

$$p = \rho \frac{\bar{R}}{M.W.} T \qquad \left[\text{thermally perfect gas}\right]$$

$$a^2 = \gamma \frac{\bar{R}}{M.W.} T \qquad \left[\text{thermally perfect gas}\right]$$

$$\frac{a}{a_r} = \frac{\rho}{\rho_r}^{(\gamma-1)1/2} = \frac{p}{p_r}^{(\gamma-1)/2\gamma} \qquad \left[\begin{array}{l}\text{isentropic flow}\\ \text{thermally and calorically}\\ \text{perfect gas}\end{array}\right]$$

Substitution in (2) yields:

$$\frac{dp}{du} = \pm \left[\frac{\bar{R}}{M.W.} \frac{Tr}{\gamma p_r^2}\right]^{-1/2} \left[\frac{p_r}{p}\right]^{-(\gamma+1)/2\gamma} \qquad (3)$$

Assuming a given reservoir pressure and a fixed pressure ratio, it can be noted that an increase in reservoir temperature or a reduction in γ will increase the velocity gain for a given pressure loss. Due to the limited range γ may vary, the initial temperature becomes the important quantity. It can also be seen that a decrease in gas molecular weight will produce a larger velocity gain. This is entirely logical if one considers the fact that a portion of the propellant gas must be accelerated to the projectile velocity. The higher the molecular weight, the more energy required to accelerate the gas and the less energy available to accelerate the projectile. For this reason a low molecular weight gas such as helium or hydrogen is the best choice for a propellant gas.

One other important result can be obtained by examining the characteristic equations as they apply here. It can be shown, that,

$$- \ln \frac{p}{p_r} = \frac{u}{a_r} \qquad (4)$$

where a_r is the speed of sound in the reservoir. If the flow velocity, u, is much less than the speed of sound in the reservoir the pressure ratio, p/p_r, will be small. Therefore another desirable propellant characteristic is that it have a high speed of sound. Again from a logical point of view, this simply means that a gas with

a high initial speed of sound can better transmit pressure increases to the projectile base.

Various other important conclusions which deal with infinite versus finite length reservoirs, chambrage and other geometrically related variables can be noted. However since this paper ultimately considers a fixed gun geometry, the effect of these other factors will be omitted in this discussion.

2.3 The Two Stage Light-Gas Gun

Even though the points made so far have been based on simple models and theory, they may be qualitatively carried over to the highly complex two-stage gun. The piston-compressed hydrogen or helium can be thought of as the reservoir mentioned above. Thus the two-stage gun can be considered as a simple gun in which the initial reservoir conditions vary.

How these reservoir conditions should be varied has been a point of some debate in the past. Berggren and Reynolds[2] group piston-compression light-gas guns into two main types according to the manner in which the propellant gas is compressed and heated. In one type the piston velocity is less than or on the order of the speed of sound in the propellant gas. This yields a nearly isentropic compression. In the other type the piston velocity is much greater than the propellant speed of sound producing strong shock waves which traverse the propellant gas, compressing and heating it. This type is called a shock-compression gun. The majority of laboratory guns

are hybrids of each type; the type of cycle being dictated by the combination of loading parameters chosen. It becomes necessary to class a particular gun in one of these two groups in order to choose an appropriate model for theoretical calculations.

2.4 Theoretical Prediction Methods

As with the guns themselves the methods for analyzing them can be classified by their assumptions and resulting complexity. A comparative study was conducted at the Ballistic Research Laboratory (BRL) by Baer and Smith[5]. Four particular mathematical models have predominated in gun research, and these were the ones chosen by BRL for comparison. They are, listed in the order of increasing complexity,

(1) Charters' Method

(2) Simple Isentropic Compression Method

(3) Richtmyer-Von Neuman "q" Method

(4) Method of Characteristics.

A comparison of the various assumptions used in each theory is given in Table I (taken from reference 5).

The simplest model, first developed by Charters[4] at NASA-Ames, consists of a set of simultaneous algebraic equations which may be solved using a desk computer. The predicted velocities agree well with experimental results at low levels of performance, but deviate significantly in performance regimes of the most interest.

The simple isentropic compression method involves a set of

TABLE 1

ASSUMPTIONS USED IN LIGHT GAS GUN PREDICTION METHODS

	CHARTER'S METHOD	SIMPLE ISENTROPIC COMPRESSION METHOD	RICHTMYER-VON NEUMAN "q" METHOD	METHOD OF CHARACTERISTICS
Light Gas Thermodynamics	Ideal gas Constant specific heat	Ideal gas Constant specific heat (Can use real gas equation of state)	Ideal gas Constant specific heat (Can use real gas equation of state)	Ideal gas Constant specific heat (Can use real gas equation of state)
Frictional Loss Projectile & Launcher Bore	Assumed negligible	Considered as a function varying with projectile travel	Considered as a function varying with projectile travel	(Unable to consider launcher conditions)
Frictional Loss Piston & Pump Tube	Assumed negligible	Considered as a function varying with piston travel	Considered as a function varying with piston travel	Considered as a function varying with piston travel
Frictional Loss Gas & Pump Tube Gas & Launcher Tube	Assumed negligible	Assumed negligible	Assumed negligible	Assumed negligible
Gas Ahead of Projectile?	No Evacuated bore	No Evacuated bore	No Evacuated bore	(Unable to consider launcher conditions)
Gas Flow in Nozzle	———	Subsonic and sonic flow in nozzle	Subsonic to sonic flow in nozzle	(Unable to consider launcher conditions)
Gas Flow in Pump Tube	No flow Isentropic compression of gas	Some arbitrary fraction of piston velocity	Sonic or supersonic flow with shock waves	Sonic or supersonic flow with shock waves
Gas Flow in Launcher Tube	Rarefaction caused by initial motion of projectile and reflected off piston does not catch up with proj.	Some arbitrary fraction of projectile velocity(used also an empirical function)	Sonic or supersonic flow with shock waves	(Unable to consider launcher conditions)
Heat Losses from Gas to Pump Tube or Launcher Tube Walls	Assumed negligible	Assumed negligible	Assumed negligible (Can be inserted in equations)	Assumed negligible (Can be inserted in eq's but with difficulty)
Propellant Driver Gas for Piston	Propellant burnout occurs before piston moves. Isentropic expansion of propellant gas as piston moves.	Propellant burnout occurs after piston moves. Gun Interior Ballistics Equations used.	Propellant burnout occurs after piston moves. Gun Interior Ballistics Equations used.	Propellant burnout occurs after piston moves. Gun Interior Ballistics Equations used.

simultaneous, ordinary nonlinear differential equations with time as the independent variable. The method is described in detail in a subsequent report by Baer and Smith[6]. The method eventually used for this paper is essentially the same as the simple isentropic compression method with the derivation of the finite difference equations being slightly different. A complete description of the theory used for this report will follow the literature survey.

Perhaps the most widely used technique is the Richtmyer-Von Neuman "q" method. In this method a set of simultaneous nonlinear ordinary differential equations and partial differential equations of the hyperbolic type are solved. Time and Lagrangian particle coordinate are the independent variables. The primary advantage of this model is that shock waves are accounted for in the pressure-time history of the pump tube. A detailed description of this technique can be found in references 6 or 7.

The last and most complicated method is a characteristic analysis. When strong shocks must be considered, solutions can only be obtained with the use of a third characteristic direction representing particle paths along which the entropy is constant. Although this method has been used successfully for a great number of other fluid dynamic problems, computer storage limitations and exceedingly long computation times have prevented detailed gun analysis based on this method.

An important consideration and one which played a part in the choice of the method to be used for this paper is the required

computation time for each method. This varies from Charters Method which does not require the use of a computer to the method of characteristics which can exceed the capabilities of many computer systems. The "q" method is within the capability of most machines, but requires a good deal more computing time than the simple isentropic compression method. During this study, a program based on the simple isentropic compression method took less than 1 minute of computing time on an IBM 360/65 computer system. However, in order to satisfy the assumptions, this method is limited to gun cycles which are characterized by low piston velocities. Reference 6 gives an excellent comparison of the Richtmyer-Von Neuman method versus the Isentropic Compression model. The basic conclusion was that the isentropic compression model is adequate for gun cycles which do not violate the basic assumptions of the theory while the "q" method gave good results for all gun cycles.

2.5 Previous Parametric Studies

A number of laboratories around the country have conducted and published results of parametric studies of light-gas guns.[8,9,10] In many cases the results are limited, in a quantitative sense, to only those guns operated by the particular laboratory. Of greater interest to this report is the qualitative observations coming out of these parametric studies. Since the two-stage cycle deals with the interaction of a large number of variables the only practical method for conducting a parametric study is to develop a computer routine capable

of accurately predicting gun performance. In assessing the conclusions of a particular study, the computer method used (See Section 2.4) and the assumptions made for that method should be considered first.

The first step in any parametric study is to identify the parameters of interest. As mentioned in the introduction, these may be classified into two groups: geometric variables and loading conditions. Again the discussion will be limited to results obtained by varying only the loading conditions. The following parameters comprise the variables of interest:

(1) Initial gas conditions

(2) Piston velocity (or powder charge)

(3) Model release pressure

(4) Piston mass

The effect of varying each is discussed in Collins, Charters, Christmar, and Sangster[8] and in a more recent summary by Berggren and Reynolds[2]. Each of these reports utilize the Richtmyer-Von Neuman "q" method, which is recognized as the most accurate computer solution to the gun problem.

Initial Gas Conditions

Once a particular propellant gas is chosen the molecular weight and the ratio of specific heats, γ, are specified. Only two gas variables remain which may be adjusted: the mass and the initial temperature. The mass of gas is directly related to the initial pressure,

so the latter parameter becomes the variable of practical interest.

Reference 2 considers a simple isentropic compression in a constant diameter closed-end pump tube and develops the following

$$\frac{dp}{dt} = \frac{\gamma A U}{V_{r_o}} \left[\frac{p}{p_{r_o}}\right]^{1/\gamma} p \qquad (5)$$

where V_{r_o} is the initial reservoir volume and U is the piston velocity. Equation (5) is at least indicative of the rate of change of pressure in the initial phases of the gun cycle when projectile motion is small. The pressure gradient represented by equation (5) will be referred to as the "pumping rate".

A lower initial pump tube pressure, p_{r_o}, will result in a higher pumping rate assuming the piston velocity, U, and the pump tube pressure, p, are considered to have particular values. The rate of pressure rise is also a function of p, rising more rapidly as the pressure level increases. Assuming the projectile is released at a particular pump tube pressure, an increase in the rate of pressure rise will cause the projectile to begin its motion earlier in the launch cycle, well before the piston has come to rest in the transition section (refer to Figure 2). As the piston continues to compress the light gas, the pressure felt by the projectile is sustained at a higher average value which results in a high muzzle velocity. It might appear that an easy way to achieve high muzzle velocities would be to assure the initial pump tube pressure of the light gas is low. However, a practical limit exists below which there is not

a sufficient quantity of gas to maintain substantial base pressures for extended distances of projectile travel.

According to equation (3), an increase in reservoir initial temperature should provide a marked increase in muzzle velocity by raising the final reservoir temperature. A report by Stephenson and Anderson[10] showed that by increasing the initial pump tube temperature from 300°K to 600°K an increase in muzzle velocity of 3,000 ft/sec could be expected.

Piston Velocity

The piston velocity has a strong influence on the projectile base pressure history. During early portions of the pump cycle the pumping rate is a direct function of the piston velocity (See equation 5). By proper selection of the propellant charge, the initial rate at which pump tube pressures rise at the onset of projectile motion may be controlled. Likewise, by choosing the proper piston mass, the deceleration of the piston, and thus the decrease in pump tube pressure, can be controlled. To obtain maximum projectile velocities the pump tube pressure must change in a specific manner. Thus a matching process between parameters influencing pressure increases or decreases must take place to achieve optimum performance. Reference 2 shows, however, that a match yielding constant projectile base pressure cannot be obtained.

The choice of how the piston velocity will vary is basically a choice of whether the compression process will be a shock compression

or an isentropic compression process. At high piston velocities the process is essentially a shock compression while at low velocities the process becomes more like a simple isentropic compression.

Projectile Release Pressure

The importance of projectile release pressure becomes evident when considering the timing of a particular gun cycle. It is usually desirable to release the projectile at a particular point in the compression cycle. The compression cycle, however, is characterized by a series of sharp pressure peaks rather than a smooth increase in pressure. Therefore a diaphragm or break valve must be chosen so that the projectile will not be released prematurely. It has been shown that cycles involving high pump rates and/or high mass projectiles are relatively insensitive to model release pressure. This is due to the projectile not moving sufficiently far into the launch tube to seriously influence the pressure rise in the pump tube.

Piston Mass

Normally the piston reaches a constant velocity before the projectile is released. The gunpowder propellant gas has expanded to a low pressure and does not add significantly to the energy of the piston once constant velocity is achieved. Therefore the piston must have sufficient kinetic energy to compress the light gas in the desired manner. One key influence is the piston mass. If too light, the piston decelerates too quickly, thereby reducing the pumping rate.

A moderately heavy piston maintains a high pump rate towards the end of the launch cycle resulting in a high overall base pressure on the projectile. If too heavy, the piston requires an unreasonable amount of energy during acceleration which lowers the piston's terminal velocity, thereby again reducing the pumping rate.

CHAPTER III

THEORETICAL DISCUSSION

3.1 General

In a mathematical sense the muzzle velocity, U_m, of a gun may be expressed as,

$$U_m = u(a, b, c, d, \ldots)$$

where a, b, c, d, ... = gun parameters, and

$$dU_m = \frac{\partial u}{\partial a} da + \frac{\partial u}{\partial b} db + \frac{\partial u}{\partial c} dc + \ldots$$

To be able to predict the change in muzzle velocity due to a change in one or more of the gun parameters a value for each partial derivative would be required. By holding all except one parameter constant it should be possible to determine to what degree that parameter influences muzzle velocity.

For the two stage light-gas gun this is difficult to achieve. An obvious method would be to perform a series of tests using a particular gun system carefully holding certain parameters constant while varying others. This would be continued until all combinations were tested. If only two or three parameters are involved this could be accomplished quite easily but when considering the effect of many parameters the purely experimental approach becomes time consuming and inefficient.

For this reason all parametric studies found in the literature as well as this thesis require the use of a prediction technique capable of simulating gun performance to some degree of accuracy. As was mentioned earlier the Richtmyer-Von Neuman "q" method has received widespread acceptance as the most general and accurate theory on which to base a particular optimization study. The simple isentropic compression method while limited to primarily isentropic compression type guns (See Section 2.3) has found use by many laboratories for initial qualitative studies. The computational economy of the simple isentropic method is an essential feature. This method was chosen for use in this study for both economy and simplicity at the sacrifice of some degree of accuracy.

3.2 The O.K. Gun Code

Rather than develop an original program it was decided to tailor a program written by Otto K. Heiney, AFATL, to this problem. The solution is based on the simple isentropic compression method in which the equations of motion of the projectile and piston along with simple gas relationships are used to solve for variables assumed to be functions of time only. The assumptions used include:

(1) The propellant gases are ideal gases with constant specific heat ratios (provision is made in the program for using the Noble-Abel "covolume" equation of state if desired)

(2) Frictional effects are negligible

(3) A perfect vacuum exists ahead of the projectile

(4) The kinetic energy of the propelling gas may be represented by some fraction of that gas moving at the piston or projectile velocity.

(5) An isentropic compression occurs in the pump tube with some heat loss being allowed and considered proportional to the square of the projectile velocity.

(6) The burning behavior of the gunpowder propellant is assumed to be adequately described by Vielle's model.

Figure (4) illustrates the computer program logic. After defining and initializing the various program variables, the computer enters a time loop which calculates such quantities as velocities, temperatures, and pressures for successtive time steps until the projectile exits the barrel. This loop includes steps 3 through 10 in Figure (4). In order to insure that the piston or projectile are not allowed to accelerate to a velocity which would cause instability in the finite difference form of the equations, an iterative time increment loop is nested within the routine (labeled as steps 6a through 6e in Figure (4)). Pressures and temperatures are updated from one time plane to the next through the use of expressions for the rate of change of pressure and temperature in both the powder gas and light gas. In the following section, these rates and the supporting theory for the program will be discussed.

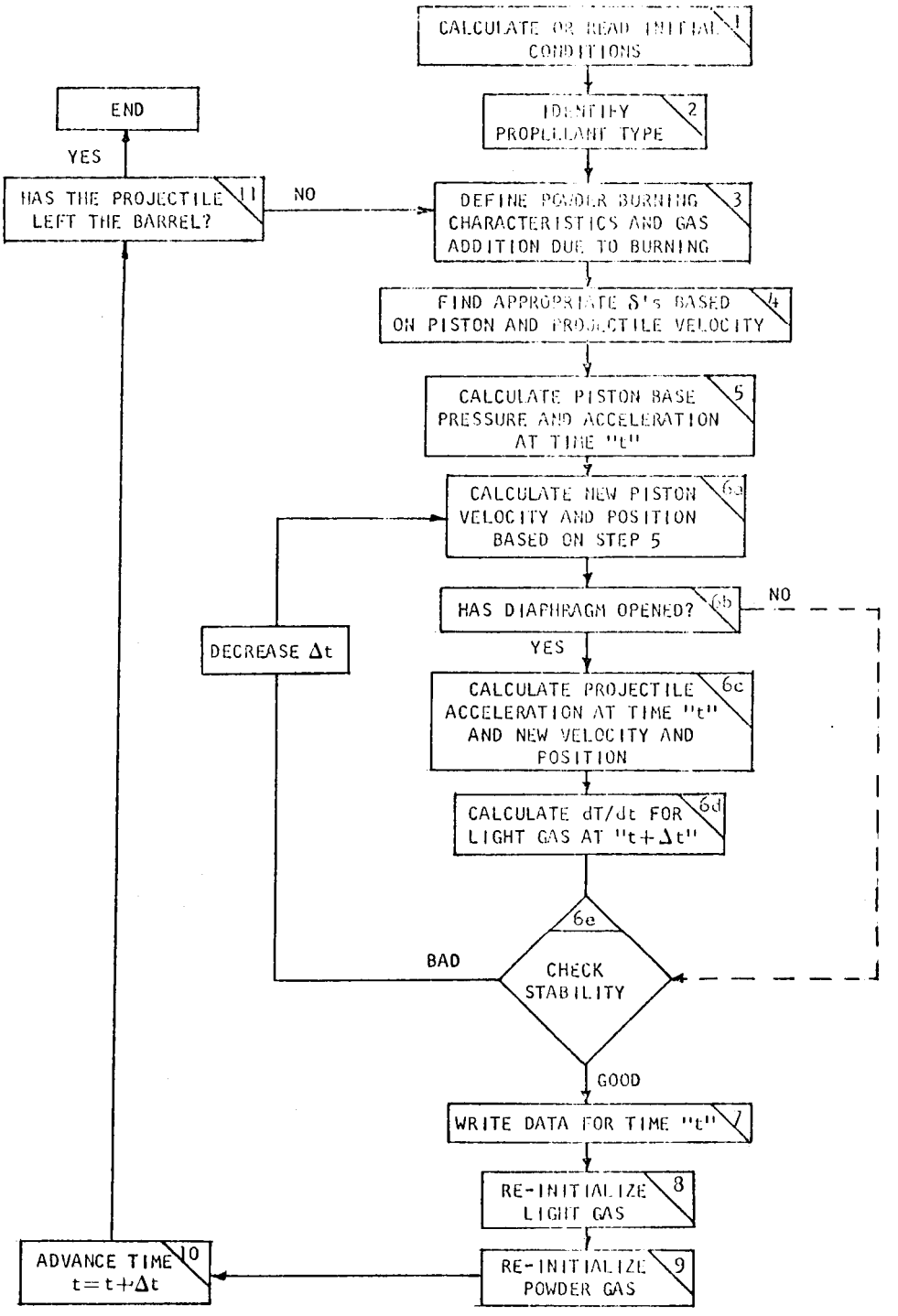

FIGURE 4: O.K. CODE LOGIC DIAGRAM

3.3 Program Theory

The approach to the ballistic problem by O. K. Heiney is essentially an energy balance where the energy put into the system is equated to the energy lost by the system. Figure (5) illustrates the two-stage gun with two energy balance systems outlined. The gun is divided into two systems; system "A" consists of the powder charge, powder gas, and piston while system "B" consists of the light gas and projectile. The work of the piston on system B is accounted for by changes in the internal energy of the system. An isentropic compression is assumed as the volume of system B is decreased due to piston motion. This compression results in an increase in temperature thus increasing the internal energy.

The approach to each energy system is basically the same. Thus, rather than present an analysis of both, only system B will be analyzed (Reference 11 presents an analysis applicable to system A). The following energy terms may be defined:

E_1 = the change in internal energy of the light gas due to compression by the piston

E_2 = the kinetic energy of the projectile

E_3 = the heat loss to wall

E_4 = energy to accelerate a portion of the light gas to the projectile velocity.

Looking at each term separately,

E_1: The change in internal energy may be written as

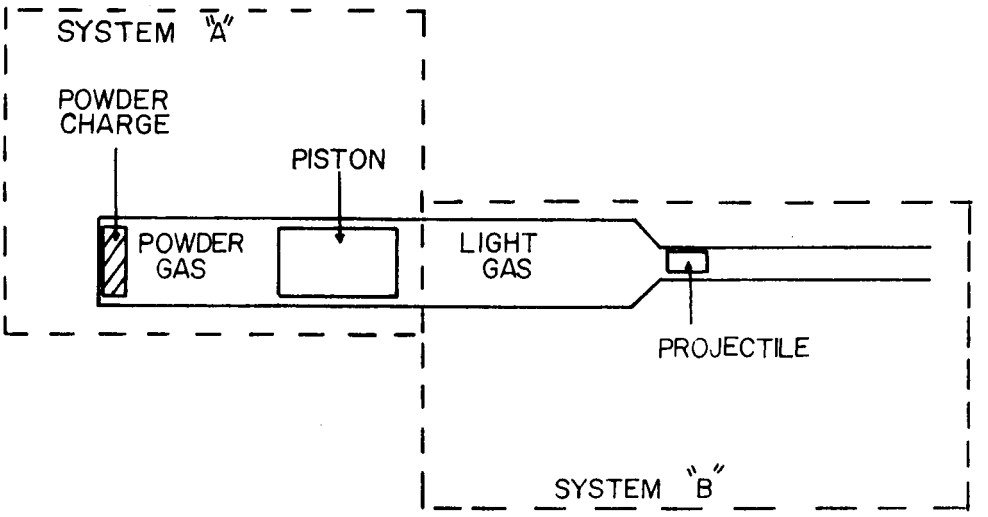

Figure 5 Energy Balance Systems

$$E_1 = M\, C_v\, (T_o - T_f) \tag{6}$$

where T_o = average initial light gas temperature

T_f = average final temperature

M = gas mass

from the Noble-Abel equation of state,

$$p_f \left(\frac{V_f}{M} - \eta \right) = RT_f \tag{7}$$

Define,

$$V' \equiv \frac{V_f}{M} - \eta \tag{8}$$

Equation (6) becomes,

$$E_1 = \frac{MRT_o}{\gamma - 1} - \frac{p_f V'}{\gamma - 1} \tag{9}$$

Since the program advances in time, the initial temperature can be taken as the temperature at time t while the final conditions are at $t + \Delta t$. Therefore,

$$E_1 = \frac{MR}{\gamma - 1} \quad T_t \quad - \frac{1}{\gamma - 1} \quad pV'_{t + \Delta t} \tag{10}$$

E_2: The projectile kinetic energy is,

$$E_2 = \frac{1}{2} M\, u^2 \tag{11}$$

where M = projectile mass

u = projectile velocity at $t + \Delta t$.

E_3: The heat loss is assumed proportional to the projectile velocity

squared,

$$E_3 = \frac{1}{2} \beta M_a u^2 \tag{12}$$

where m_a = psuedo mass defined as the projectile mass plus some fraction of the light gas which must be accelerated to the projectile velocity.

$$M_a = M_{proj} + \frac{M_{gas}}{\delta} \tag{13}$$

E_4: The kinetic energy of the light gas may be represented by,

$$E_4 = \frac{1}{2} M_a u^2 \tag{14}$$

The primary difficulty lies in choosing an appropriate value for δ. The factor δ allows the total kinetic energy of the light gas to be represented by the kinetic energy of a fraction of the gas mass moving at the projectile velocity. Heiney[12] summarizes the classical interior ballistic solution of LaGrange, who notes that at low projectile velocities the gas density can be assumed to be essentially constant along the axial direction, ie.

$$\frac{\partial \rho}{\partial x} = 0$$

This assumption permits a closed form solution for the gas kinetic energy and results in $\delta = 3$. In other words, the energy in the accelerating gas is equivalent to 1/3 of the gas mass traveling at the projectile velocity. This approximation is inaccurate, however, at velocities where the density is no longer uniform. By assuming that

a linear velocity gradient exists behind the projectile and that isentropic flow relations may be used to describe the gas flow, Heiney formulated a solution for δ as a function of projectile velocity in which the gas density is allowed to vary. For this thesis an extrapolation of Heiney's curve was used to obtain values for δ corresponding to projectile velocities up to 30,000 ft/sec, which is well above the maximum velocities predicted by the computer routine.

The energy equation may now be written as,

$$E_1 = E_2 + E_3 + E_4 \tag{15}$$

substituting (10), (11), (12) and (14) into (15) yields

$$\frac{MRT_t}{\gamma-1} - \frac{p_{t+\Delta t}V'}{\gamma-1} = \frac{1}{2}(\beta + 1) M_a u^2$$

and rearranging terms

$$p_{t+\Delta t}V' = MRT_t - \frac{1}{2}M_a (\gamma - 1)(\beta + 1) u^2 \tag{16}$$

Equation (16) may be differentiated with respect to time to yield,

$$\frac{dp}{dt}_{t+\Delta t} = - \frac{p}{V'}\frac{dV'}{dt} + \frac{MR}{V'}\frac{dT}{dt}_t - \frac{M_a(\gamma-1)(\beta+1)u}{V'}\frac{du}{dt}$$

Note, $\frac{dV'}{dt} = A_2u - A_1U$

where A_2 = projectile base area

A_1 = piston base area

U = piston velocity at $t + \Delta t$

so,

$$\left(\frac{dp}{dt}\right)_{t+\Delta t} = \frac{p\,A_1 U}{V'} - \frac{p\,A_2 u}{V'} + \frac{MR}{V'}\left(\frac{dT_t}{dt}\right)_t$$

$$- \frac{M_a(\gamma-1)(\beta+1)u}{V'}\frac{du}{dt} \qquad (17)$$

Also if the process is isentropic, the rate of change of temperature is given by:

$$\left(\frac{dT}{dt}\right)_{t+\Delta t} = \frac{\gamma-1}{\gamma}\frac{T}{p_t}\left(\frac{dp}{dt}\right)_{t+\Delta t} \qquad (18)$$

By using equations (17) and (18) along with initial conditions, the pressure and temperature may be calculated for any time plane.

The pressure and temperature which are computed are "average" values. The base pressure on the projectile is the quantity which controls projectile motion and becomes the desired quantity.

A pressure ratio based on isentropic expansion theory is

$$\frac{p_b}{p_o} = 1 + \frac{\gamma-1}{2g}\left[\frac{u^2}{\gamma RT}\right]^{-\gamma/\gamma-1}$$

where T = average light gas temperature.

This ratio allows the base pressure to be calculated in terms of the total or stagnation pressure, p_o. Since the piston is at or near the end of the compression cycle when the projectile is released, steady state conditions may be assumed. The total chamber pressure may be approximated by the average pressure obtained from the energy

balance. Therefore,

$$\frac{p_b}{p_{ave}} = 1 + \frac{\gamma-1}{2g}\left[\frac{u^2}{\gamma RT}\right]^{-\gamma/\gamma-1} \tag{19}$$

and the base pressure may be calculated at each time plane.

By referring back to Figure (4) in Section 3.2 it can be seen that a stability criteria was required in order to use the equations in the form presented above. The problem was primarily concerned with limiting the motion of both the piston and projectile so the pressures would remain positive and stable over each time interval. In each case an arbitrary reference distance was chosen. The time interval required for a pressure disturbance to propagate across this reference distance was determined through the use of the disturbance velocity. That is,

$$\frac{\Delta X_{ref}}{\Delta t} = U_{disturbance} = U_{gas} + a$$

or,

$$\Delta t = \frac{\Delta X_{ref}}{U_{gas} + a} \tag{20}$$

The gas velocity, U_{gas}, was taken to be the velocity of the gas bordering the projectile or piston. Therefore the gas velocity corresponded to the projectile or piston velocity. The speed of sound, a, was calculated using the average temperature of the light gas.

On each time plane the time increment was compared to the value

given by equation (20). If too large, the increment would be reduced and the computer would re-calculate all terms influenced by the reduction. The comparison and re-calculation would continue until the time increment was smaller than or equal to the value given in equation (20).

The reference distance chosen for the "piston motion" criteria approximates the distance from the piston face to the end of the pump tube (See Figure (6) in Section 3.4). Only as the piston nears the end of its travel in the pump tube does this criteria override the time increment used by the computer program. The reference distance for the "projectile motion" criteria was arbitrarily chosen to correspond to the diameter of the launch tube bore.

3.4 Gun Modeling

Figure (6) illustrates the manner in which the Texas A&M gun was modeled for computational purposes. All dimensions were taken from construction drawings supplied by NASA. The actual powder chamber configuration is much more complex than the one chosen in the model. In reality the powder chamber consists of a tapered hole, sized to accept a .458 magnum cartridge, opening into a chamber which has a converging nozzle to the pump tube inside diameter. The volume of the chamber was the variable required to initialize the program. An imaginary chamber having the pump tube diameter and a psuedo length, L_1, was assumed so as to have the same volume as the actual powder chamber.

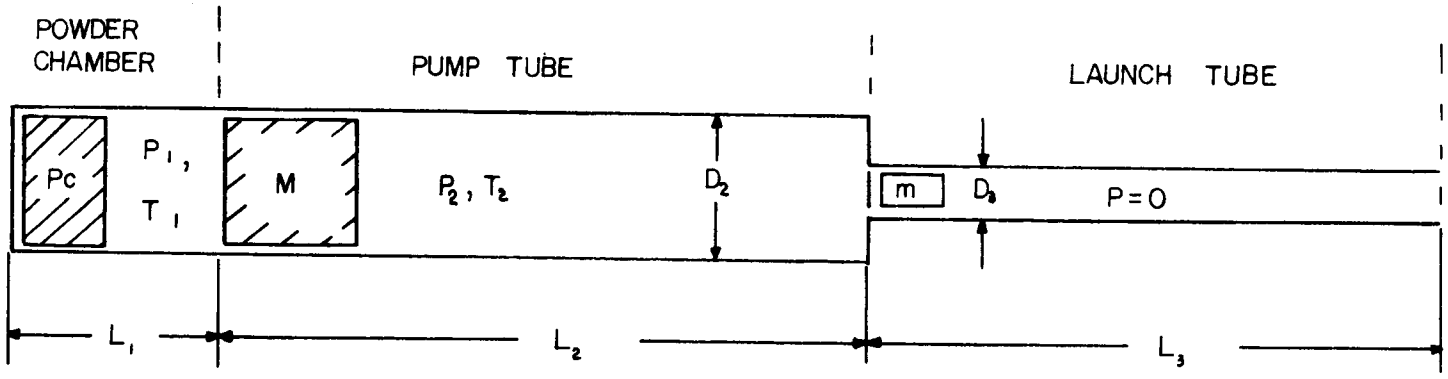

GEOMETRIC CONSTANTS

$D_1 \cong D_2 = 0.320$ in

$D_3 = 0.085$ in

$L_1 = 14.75$ in

$L_2 = 17.0$ in

$L_3 = 9.0$ in

TYPICAL LOADING PARAMETERS

$P_1 = 15$ psia

$P_2 = 50-175$ psia

$T_1 = T_2 = 293°K$

$M = 1.5 - 5.0$ g

$m = 0.010 - 0.040$ g

$Pc = 2.0 - 3.5$ g

Figure 6 Model of the Texas A&M Light Gas Gun

Not shown in Figure (6) is the manner in which the powder charge was assumed to burn. The rate at which gas is released by a burning propellant can be expressed as (using Vielle's formulation),[11]

$$\frac{dN_B}{dt} = r\, S_B\, \rho_p \qquad (21)$$

where N_B = mass of gas released

ρ_p = propellant density

As is popular in the solid rocket industry, an exponential burning rate, r, was chosen of the form:

$$r = B\, P^n \qquad (22)$$

where P = chamber pressure

B,n = constants

Table II gives the properties for double base, Nitro cellulose-Nitroglycerin propellants as obtained from Sutton, Rocket Propulsion Elements[13].

By taking r = 0.6 and n = 0.5 the constant B in equation (20) was determined. The equation used was,

$$r = 0.0189\ (P)^{0.5}\ .$$

In addition the propellant was assumed to be made up of small, uniformly shaped disks with an average web thickness, w, of 0.01 inches. Assuming negligible loss in area due to burning along the circumference, the total burning area for all the disks will be

$$S_B = \frac{m}{w\rho_p} \tag{23}$$

where m = total mass of disks

w = disk thickness

ρ_p = density of the propellant

With r, S_B, and ρ_p determined, the manner in which the propellant burns can be incorporated into the program.

TABLE II TYPICAL POWDER CHARACTERISTICS

Property	
Adiabatic Flame Temp.	3800-5200^o F.
Ave. Molecular Wt.	22-28
Specific Heat Ratio	1.21-1.25
Burn Rate at 1000 psi	0.6-0.9 in/sec
Specific Weight (ave.)	0.058 lb/in^3
Burn Rate Exponent, n	0.1-0.8

3.5 Program Results

The results of the computation are illustrated in Figures (7) through (12) for some arbitrary test cases. The parameters of most interest were those which could easily be varied through a wide range during the subsequent experimental study. These are:

(1) Pump tube pressure

(2) Piston mass

(3) Powder charge, and

(4) Diaphragm burst strength.

Projectile mass was held constant. Equation (1) in Section 2.2 predicts projectile velocity to be a simple and predictable function of projectile mass. The conclusions which can be drawn from the figures basically conform to those offerred in Section 2.5.

An increase in muzzle velocity with decreasing initial pump tube pressure is illustrated in Figure (7). Results for two powder charges are shown. The curves indicate the same trend as disucssed in Section 2.5. The primary cause of the increase is an increase in the rate at which pump tube pressures rise. Higher maximum pressures and temperatures are predicted in the pump tube which, in turn, tend to increase the average projectile base pressure.

It should be noted that these computations were intended to be qualitative in nature and not quantitative predictions of actual gun performance. The assumptions and simplifications make the numbers much less important compared with the trends they indicate. Figure (8) provides a good example. Here the influence of piston mass is shown to increase rapidly and then tend to level off at values above 4 or 5 grams. The experimental program, to be discussed next, verified this trend in actual gun data.

The influence of powder charge and diaphragm burst pressure are illustrated in Figures (9) and (10). The program predicted a nearly linear increase in muzzle velocity with increasing powder charge.

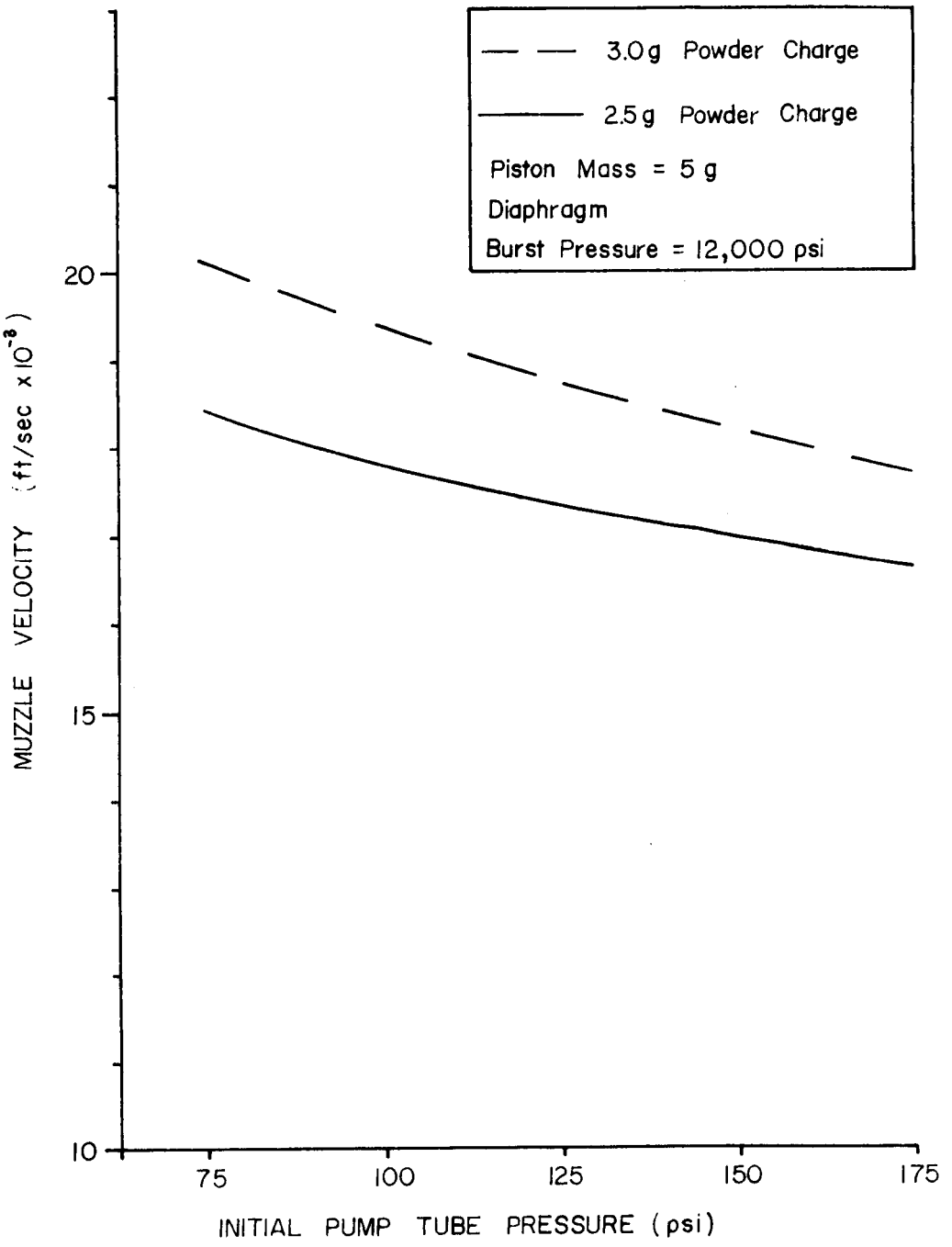

Figure 7 Theoretical Influence of Initial Pump Tube Pressure on Muzzle Velocity

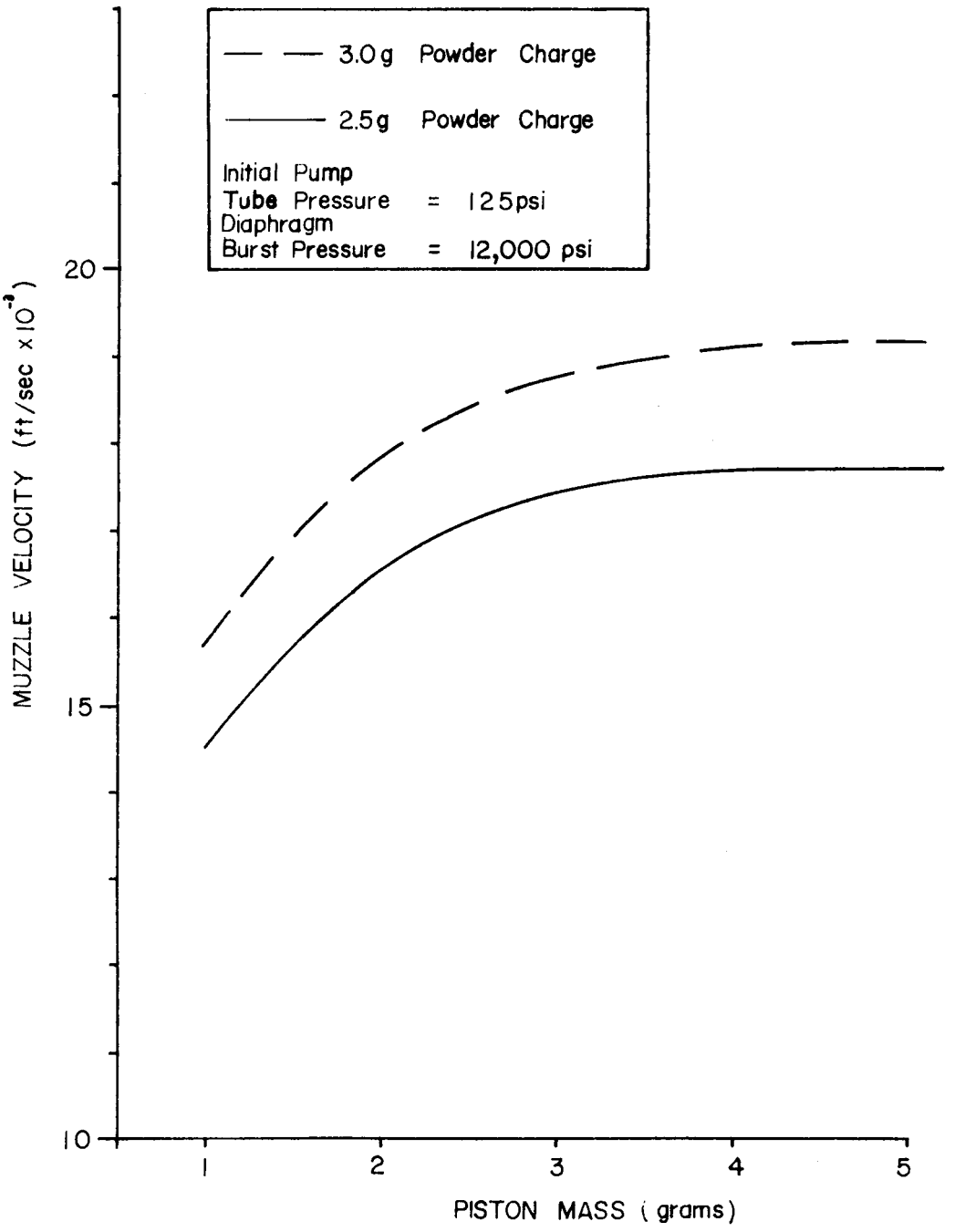

Figure 8 Theoretical Influence of Piston Mass on Muzzle Velocity

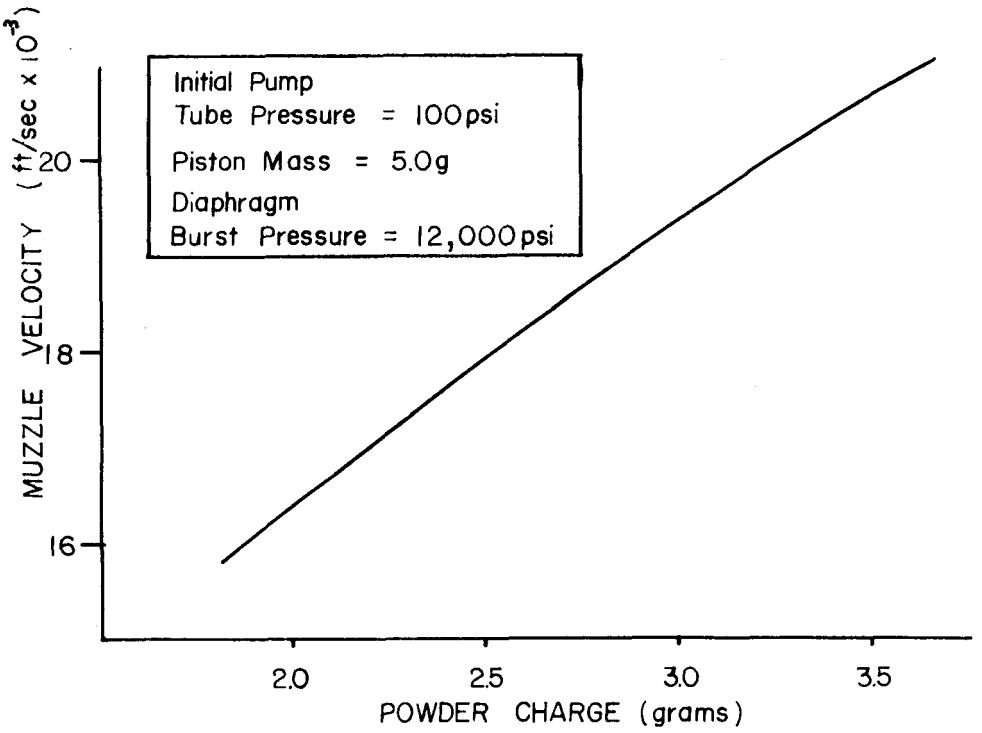

Figure 9 Influence of Powder Charge on Muzzle Velocity

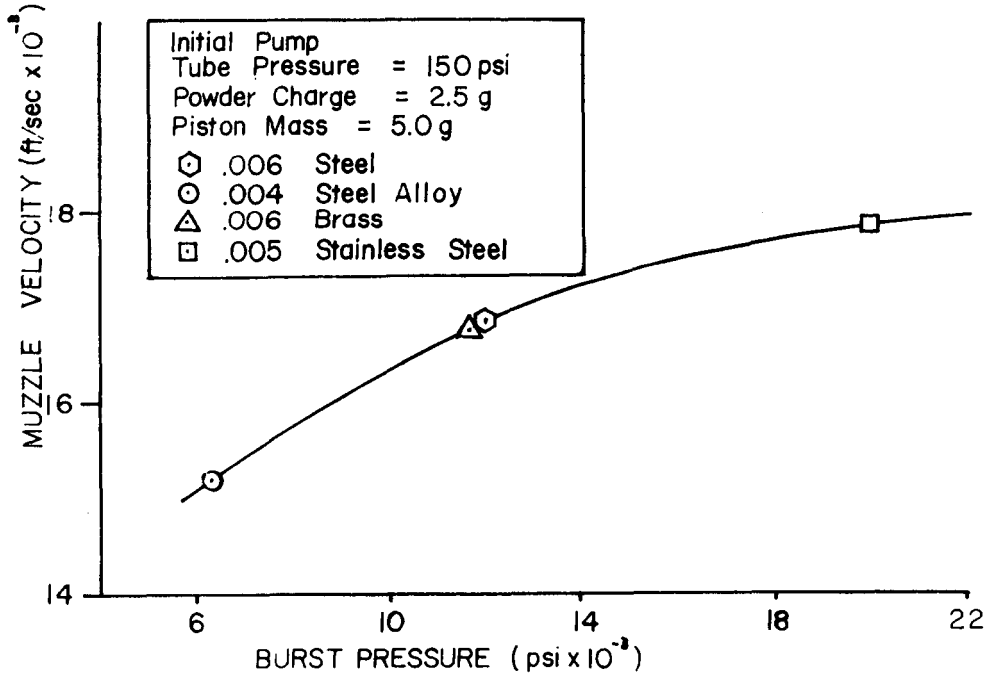

Figure 10 Influence of Diaphragm Burst Pressure on Muzzle Velocity

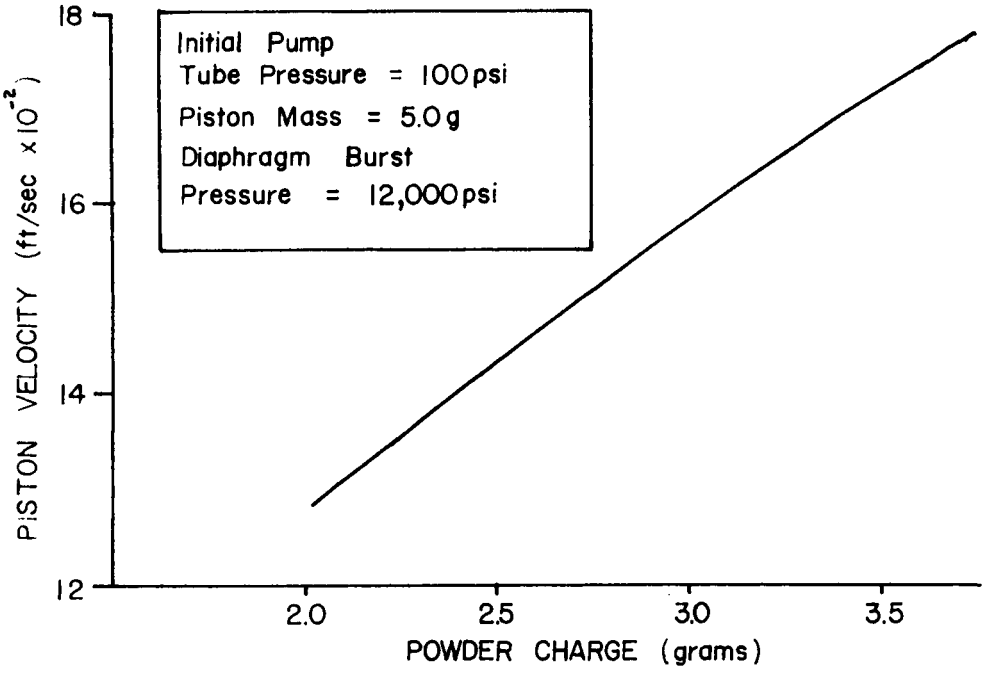

Figure 11 Influence of Powder Charge on Maximum Piston Velocity

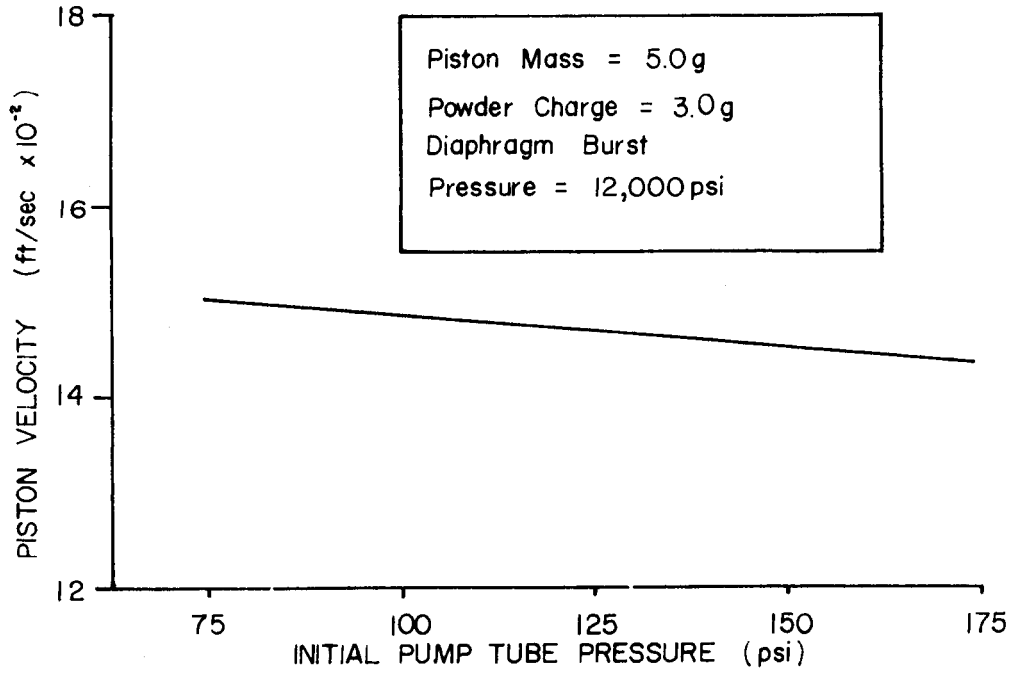

Figure 12 Influence of Initial Pump Tube Pressure on Maximum Piston Velocity

The important characteristic here is the slope of the curve. The computations predict muzzle velocity to be sensitive to powder charge more than any other loading parameter. Diaphragm burst pressure displays a strong influence at low values, but tends to decrease at high burst pressures. From a practical point of view only particular types of diaphragms are available each having their own unique burst pressure. The .005 stainless steel and .006 steel were the types used for the experiments.

One interesting comparison is illustrated in Figures (11) and (12). Here maximum piston velocity is ploted versus both powder charge and initial pump tube pressure. The piston velocity seems much more sensitive to a change in powder charge than a change in pump tube pressure. As mentioned in Section 2.5, the projectile's muzzle velocity is influenced directly by the manner in which the piston velocity varies. So the stronger dependence of muzzle velocity to powder charge rather than initial pump tube pressure is understandable.

Individual points were not plotted to obtain the graphs discussed in this section. If they had, it would be evident that the computer routine did not always predict a smoothly varying curve, but rather a kind of oscillation about a mean value. In cases where no smooth curve could be drawn through all the points, an average curve was drawn to represent the trend of the data. This failure of the program to predict smooth curves is not fully understood, but part of the explanation no doubt arises from the simplifications

involved. For example, under certain sets of input parameters the program will predict expansions to negative pressures. In these cases, it is assumed that the program is basically correct up to the point that negative pressures are predicted and that it then continues with only small error. Despite these anomalies the program does not become unstable; and generally the negative pressure occurs at the projectile base, which implies that the driving gas has been completely expanded (or "over-expanded").

CHAPTER IV

DISCUSSION OF EXPERIMENTS

4.1 General

The experimental program was intended to accomplish three goals. The first was to show the dependence of muzzle velocity on each of the primary loading parameters from a purely experimental approach. The second was to generate enough experimental data so that a comparison with theoretical results could be made. The third and final goal was to identify optimum loading parameters suggested by the previous experimental and theoretical work.

It was felt that the first two goals could be accomplished by examining the results from a single group of test firings. In this report this group is referred to as the "parametric tests". Another short series of gun firings were directed toward the third goal and will be referred to as the "optimization tests". Before discussing these various tests, a brief description of the gun and associated equipment will be given.

4.2 Description of the Gun System

The Texas A&M light-gas gun originated as a small portable system built by NASA-MSC in 1967 to use for both simulation experiments and demonstrations. The emphasis was on a small portable unit which would be self-contained. It was felt that simulations of space-

like environments would be improved if a light-gas gun could be brought on site and used to impact various components with high speed particles. At the time of inception, projectile velocities in the neighborhood of 10 Km/sec were anticipated. The gun dimensions were chosen by simply scaling down a larger gun system. After construction was complete, initial test shots indicated the performance to be significantly less than expected. As a result, the system was never utilized for the wide range of tests originally planned.

The gun consists of five separate parts which are either screwed or bolted together during gun assembly. These parts are:

(1) the firing magazine

(2) the powder chamber

(3) the pump tube

(4) the high pressure section, and

(5) the launch tube or barrel.

The firing magazine consists of a plunger-type selonoid which, when triggered electronically, strikes a firing pin. The powder chamber provides a mounting hole for a .458 Magnum rifle cartridge along with a nozzle transition into the pump tube entrance. Both ends of the pump tube are sealed with o-rings adjacent to a small feed hole located midway along the 0.320 inch diameter bore. The high pressure section provides a smooth transition from the pump tube into the launch tube, and is rugged enough to withstand the high pressures generated when the gun is fired. The 9 inch launch tube has an average 0.085 inch bore. The muzzle is mounted into a flight range

and is sealed with an o-ring so that the flight range may be evacuated. The flight range itself consists of a blast tank, a 6-foot flight tube, and an impact chamber. Additional information concerning the gun system is given in Appendix A.

Hydrogen was used as the light-gas propellant for the experiments. Hercule's type 2400 smokeless rifle powder was used to hand load either Winchester or Remington pre-primed cartridges. The pump tube pistons were machined from 3/8 in. diameter, type F polyethelene rod stock. The projectiles were machined from 1/8 inch diameter Lexan polycarbonate rod stock. Both pistons and projectiles were machined on jeweler lathes to the proper dimensions.

Two types of diaphragms were required for each gun firing. A 1/16 inch thick disk cut from phenolic sheet material was used to separate the powder chamber and pump tube. It had a measured hydrostatic break strength of 620 psi. The purpose of this diaphragm was to insure a high powder chamber pressure before piston motion was allowed. As will be mentioned in the conclusion, an increase in the strength of this diaphragm could have a significant effect on muzzle velocity. A second metal diaphragm is located between the transition section and the launch tube. This diaphragm controls the time at which the projectile is released. An independent study was conducted to determine the relative break strength of various types of metals. Table III lists the results of this study. The burst pressures listed are hydrostatic values. The actual dynamic burst pressure was assumed to be adequately described by this static measurement.

By choosing one type of diaphragm over another some control of the time of projectile release could be exercised.

TABLE III: DIAPHRAGM BURST PRESSURES

Diaphragm Type	Average Static Burst Pressure
.006 Steel (STL)	12,000 psi
.005 Stainless STL (SS)	20,000 psi
.004 Steel alloy	6,300 psi
.006 Brass	11,800 psi
2X .006 STL	24,400 psi
2X .005 SS	31,800 psi

The only gun instrumentation dealt with muzzle velocity measurement. A conventional ballistic screen technique was used. As the projectile left the barrel it would break a thin strip of ballistic paper which would, in turn, begin a counter and trigger an oscilloscope. At a known distance down range another strip of ballistic paper would be pierced by the projectile. This event stopped the counter and was displayed as a sharp change in voltage on the scope. Thus a measure of the flight time over a known distance could be obtained. In actual practice, the counter was found to be unreliable due to irregularities in the trigger signal. Figure (13) illustrates a typical oscilloscope data record. It contains a large negative

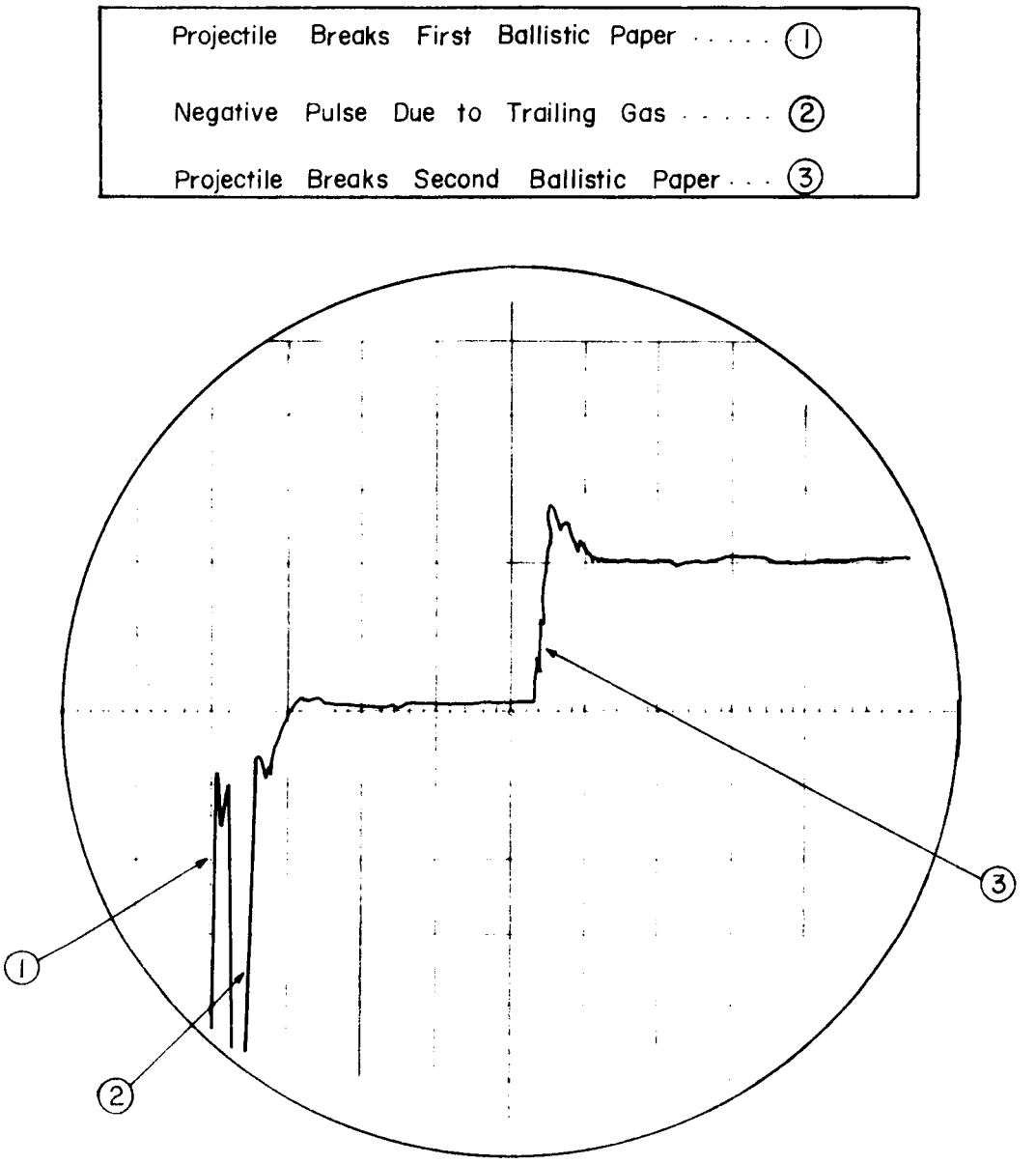

HORIZONTAL SWEEP = 100 μsec/cm

VERTICAL SWEEP = 0.5 v/cm

Figure 13 Typical Data Trace

pulse which was present in practically all the data taken. It is felt the hot gases exiting the barrel behind the projectile are responsible for this pulse.

4.3 Parametric Tests

A decision had to be made as to the values, and range of values the various loading parameters should take in order to accomplish the first two goals outlined in Section 4.1. Unfortunately, stability problems delayed the use of the computer code, so the choice of a starting point had to be made without knowing what the theoretical results would be. The parameters were chosen primarily from a convenience standpoint along with some initial estimates at what might eventually constitute the optimum set of parameters.

The piston mass, for example, was set at 1.5 grams for the beginning of the parametric tests. From the information in the literature along with previous tests conducted by NASA-MSC this appeared to be a good number. By carefully turning a section of 3/8 inch polyethylene rod stock on a jeweler's lathe a 1.5 gram piston could easily be machined. As will later be seen, this particular piston mass was really too low for good gun performance. The powder charge, initial pump tube pressure, and burst diaphragm pressure were all chosen in a similar fashion.

The test shots themselves were organized into test "series", each being identified by the values chosen for each parameter. Table IV gives a listing of each parameter, the "series" name, and

the corresponding parametric values for each series.

TABLE IV PARAMETRIC TEST SERIES

	Series			
	A	B	C	D
Parameter	Values Investigated			
Diaphragm Burst Pressure	20,000 psi	12,000 psi	12,000 psi	20,000 psi
Initial Pump Tube Pressure	50-125 psi	50-150 psi	50-162.5 psi	75-150 psi
Piston Mass	1.5 g	1.5 g	1.5 g	1.5 g
Powder Charge	2.0 g	2.0 g	2.5 g	2.5 g
Average Projectile Mass	12 mg	12 mg	12 mg	12 mg

The results of a portion of the test shots are plotted in Figures (14) and (15). Only the data which displays definite trends is plotted. Figure (14) illustrates the effect of varying initial pump tube pressure on muzzle velocity. The muzzle velocity varied little over the full range of pump tube pressures tested. This trend is typical of the majority of data taken. In comparison with theory, the experimental data fails to display a steady increase in velocity

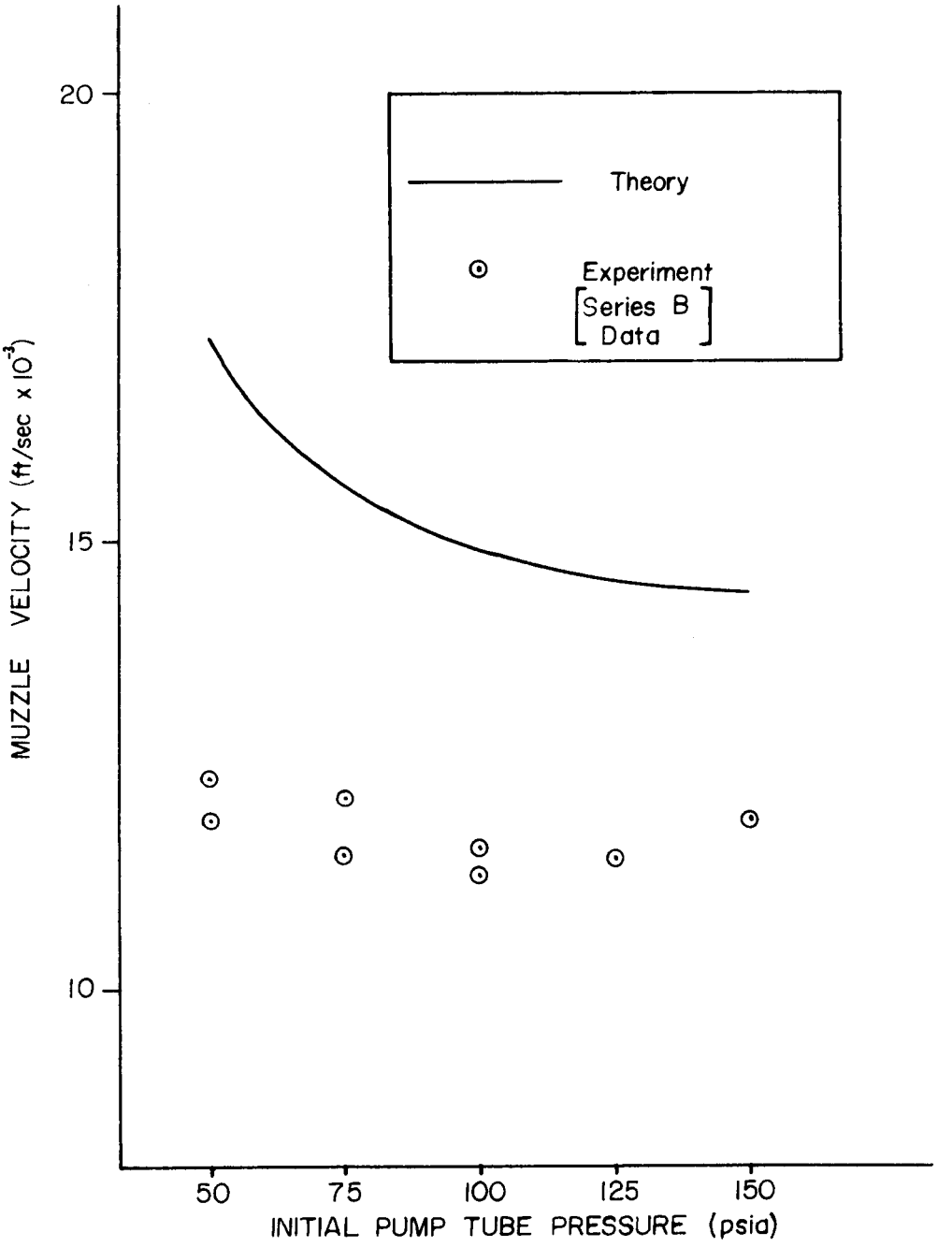

Figure 14 The Influence of Initial Pump Tube Pressure on Muzzle Velocity

with lower initial pump tube pressures. This might be expected, however, if consideration is given to the assumptions used to obtain the theoretical curve. The piston-compression process is assumed to be adequately described as an isentropic compression in which wave phenomea is neglected (See Section 2.3). As initial pump tube pressure is decreased this assumption becomes invalid due to the higher piston velocities which are involved. Strong pressure waves, even shock waves, can be expected as the retarding pressure on the piston face is reduced thus resulting in higher piston velocities. A theoretical method which takes into account the losses associated with strong pressure disturbances might provide a better match with the experimental results. On the other hand, a better choice of loading parameters than those given in Table IV may have provided a better match to the isentropic compression theory.

Figure (15) illustrates the influence of powder charge on muzzle velocity. The tests were run with a stainless steel diaphragm whose hydrostatic burst pressure was measured at 20,000 psi. As predicted by theory, an increase in powder charge produced a marked increase in muzzle velocity. A similar series of tests using a diaphragm whose hydrostatic burst pressure was 12,000 psi failed to display a definite trend. However, the optimization tests, to be discussed in the next section, also demonstrated a velocity gain due to increased powder charge. The unexpected improvement in agreement between experiment and theory for the 2.5 gram powder load shown in Figure (15) is difficult to explain. One possible explanation might be based on the

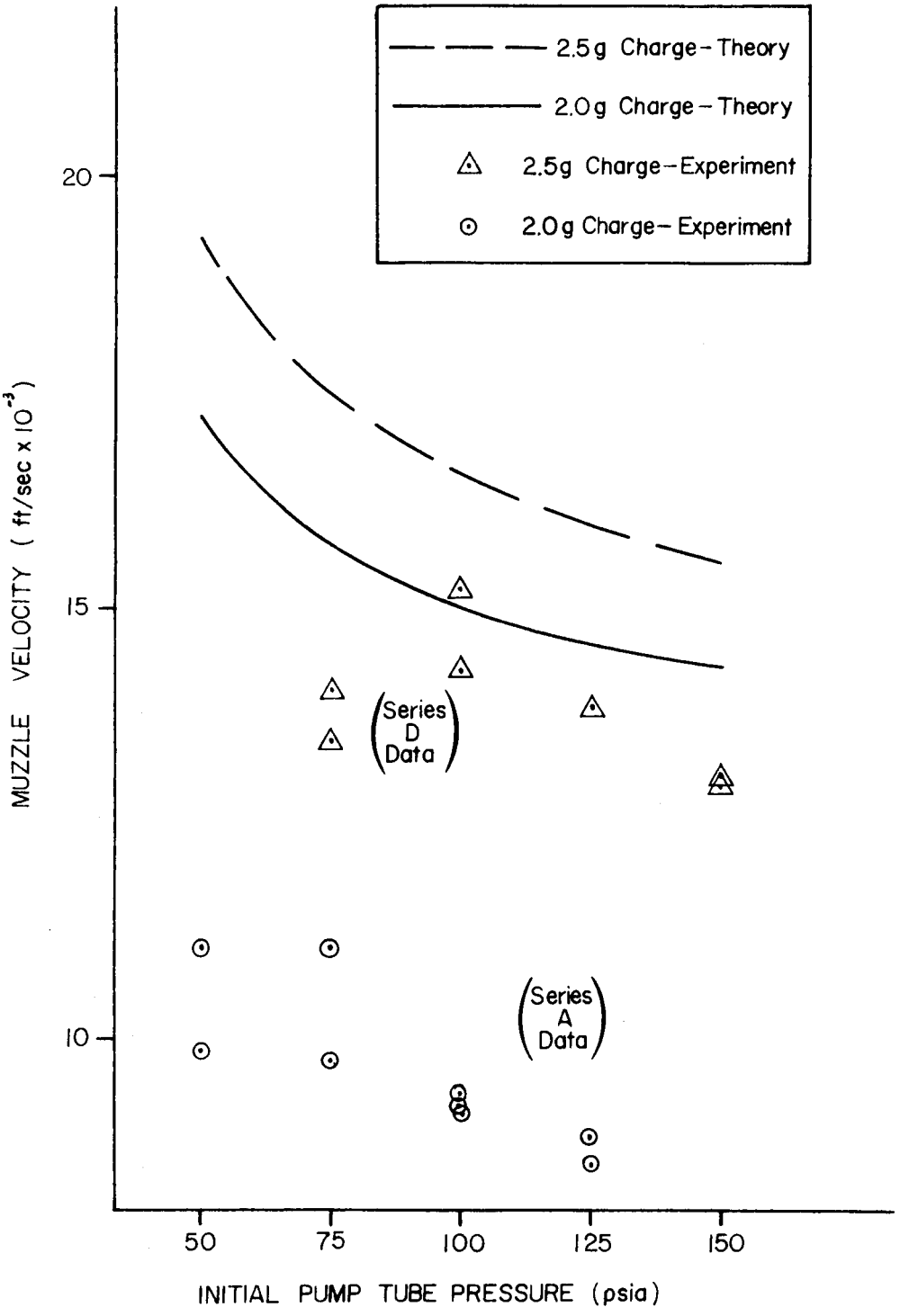

Figure 15 Exp. Influence of Powder Charge on Muzzle Velocity

way the burning behavior of the gun powder was modeled for the computer program (See Section 3.3).

At first glance, the four test series which comprise the parametric study seem to represent a rather modest test program. However a total of over 60 actual gun firings were needed to generate the data. Appendix B contains a complete table of test results. The results of the parametric tests are somewhat inconclusive and, in some respects, incomplete (A series of tests in which piston mass alone was varied was not performed). However, enough data was generated to use as a comparison with theory and enough experience gained to suggest improved combinations of parameters in order to obtain higher muzzle velocities. The goals of the tests were at least partially obtained.

4.4 Optimization Tests

From the information obtained during the parametric tests and as the results of the computer program became available, various parameter combinations appeared to be better than others. A number of gun firings were conducted in an attempt to identify an optimum set of loading parameters; that is, parameters which would yield consistently high muzzle velocities. Table V contains a list of muzzle velocities obtained from various shots during this experimental program.

The highest muzzle velocities were achieved by increasing both piston mass and powder charge. The piston mass was increased from

1.5 grams used in the earlier parametric tests to a value which varied between 3.0 to 5.0 grams. The trends indicated by the computer program (and discussed in Section 3.5) led to the increase in piston mass. The technique used to increase the mass was simply the addition of a lead plug to the rear portion of the piston. Figure (16) illustrates a typical piston both with and without the lead plug.

TABLE V MUZZLE VELOCITY INCREASES

Shot Number	Date	Muzzle Velocity
6A	6/9/72	9,300 ft/sec
21B	6/22	12,100
40C	6/29	12,900
45D	7/6	13,800
47D	7/6	15,200
56	7/16	15,900
57	7/16	16,600
55	7/11	17,900
59	7/16	19,000

The literature, theoretical results, and early experiments all seemed to indicate a strong influence of powder charge on muzzle velocity. Therefore the powder charge was increased from the 2.0 to 2.5 grams used in the parametric tests to 3.0 to 3.5 grams for the

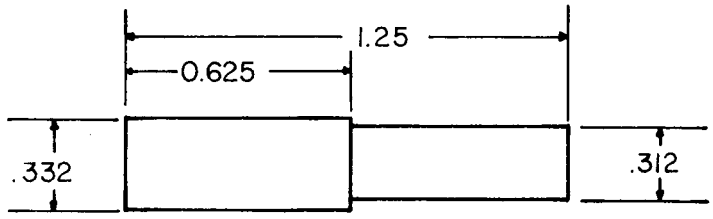

Machined From 3/8 in. Diameter Polyethelene Rod

(a) Unweighted

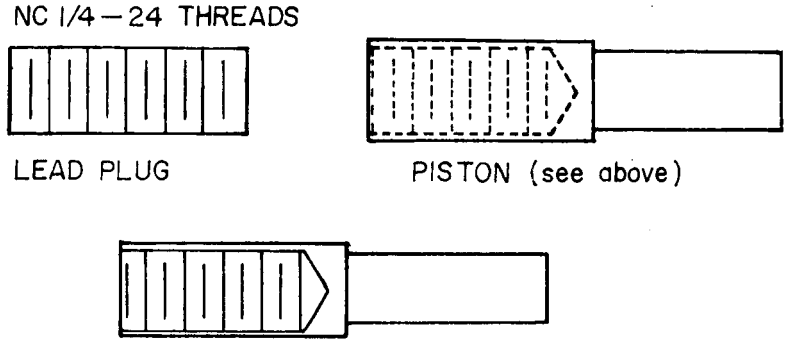

(b) Weighted

NOTE: ALL DIMENSIONS ARE IN INCHES.

Figure 16 Typical Piston Configurations

optimization study. Unfortunately, pressure leaks at the rear of the pump tube accompanied this rise in powder charge. While increasing powder charge yielded a higher velocity, the increase due to powder loads at or above 3.5 grams were negligible because of the leakage.

It was found that the velocity was higher at high initial pump tube pressures. The highest muzzle velocities were recorded at an initial hydrogen pressure of 150 psia. Shots were conducted at lower pressures but the results showed a decrease in muzzle velocity instead of the increase predicted by theory. An explanation based on possible shortcomings of the theory are discussed in Section 4.3 however other explanations may be offerred by noting sources of experimental errors.

4.5 Experimental Error

A significant spread in experimental data has been inherent in the majority of reports dealing with light-gas gun performance. The data obtained during the parametric tests of this report also displayed a wide variation despite careful attention to control the loading parameters involved. To present a full discussion of the experiments comments on possible sources of experimental error are required.

Possible errors can be associated with both the gun itself and the techniques used in obtaining the data. Perhaps the most organized way to discuss errors associated with the gun is to list some of the more obvious ones separately;

(1) Powder Chamber Leakage - Leakage at the powder chamber pump tube junction was a serious problem in a number of the test shots conducted. This was especially true when 3.0 or more grams of gunpowder were used. This leakage alters the pressure history on the piston base and therefore affects the piston velocity. As has been mentioned previously, the muzzle velocity is strongly dependent on the manner in which the piston velocity changes. No effort was made to quantitatively predict the changes in muzzle velocity due to powder chamber pressure leaks. However, in those shots in which leakage occurred the resulting muzzle velocity was always lower than in similar shots without leakage.

(2) Light Gas Contamination - Contamination of the light gas can occur from either deterioration of the gun wall due to high gas temperatures or leakage of the powder gases past the piston during the pumping cycle. While deterioration of the gun wall could occur, this source of contamination is probably negligible. The wall is exposed to very high temperatures for only an extremely short period of time. Examination of the gun from shot to shot showed no visible signs of wall deterioration. Leakage of heavy powder gases past the piston is the most probably source of contamination. A fine, black powder was observed on the flight range walls following each shot. Reference 14 reports a similar piston leakage problem which seriously degraded light-gas gun performance.

(3) Fluctuation in Diaphragm Burst Pressure - It was found during the hydrostatic burst tests (See Section 4.2) that a particular

type of diaphragm failed to break at the same pressure level from test to test. For example, the tests for the 0.006 steel yielded burst pressures from 11,300 psi to 12,600 psi a difference of over 1000 psi. Part of this variation can be attributed to experimental error, but it seems these tests demonstrate that a certain variation in pressure level at which a given type of diaphragm will burst should be expected. The effect on muzzle velocity from this variation is minor. As was mentioned in Section 2.5, the diaphragm effects muzzle velocity by controlling the time at which the projectile is released. The diaphragm breaks during a sharp rise in pressure and, thus, a small variation in break strength should not significantly influence the time at which the diaphragm bursts.

The technique used to obtain data provided an additional source of experimental error. The use of ballistic screens is an established procedure with which to measure muzzle velocity. However, since the projectile must impact each screen during flight, an energy loss can be associated with this technique. This loss becomes more significant as the mass of the projectile decreases. A typical projectile mass used for this study was on the order of 10 mg. The energy loss due to the ballistic screen technique could have seriously affected the accuracy of the velocity measurements. However by noting some previous velocity measurements obtained by NASA-MSC using high speed camera techniques, the velocity measurements used for this report were shown to fall within the same range of values. No direct correlation could be made due to differences in loading parameters used.

The reference distance between screens must also be chosen so as to not exceed the resolution of the time measurement equipment. In this study a reference distance of 7.0 ft. was chosen which provided typical flight times ranging from 300 to 600 μsec, well within the resolution of the counter and oscilloscopes used.

Finally, a comment on the effect of aerodynamic drag on the projectile will be discussed. The flight range was evacuated to less than 0.5 torr for all the test shots conducted, and calculations of drag reduction of the projectile's velocity showed a decrease of less than 10 ft/sec. Based on the manner in which the ballistic screens were broken, it did appear that the projectile tumbled during flight; but this tumbling effect was assumed to have a negligible influence on the flight time between screens.

CHAPTER V

CONCLUSION

Several conclusions may be drawn concerning the overall performance of the particular gun. Low muzzle velocities relative to other operational light-gas guns have been predicted utilizing the principal of isentropic compression of the driver gas. Since these velocities are also achieved experimentally, it may be concluded that the gun undergoes a nearly isentropic compression process during the launch cycle.

The highest muzzle velocities reported by other guns are achieved by a shock compression process. Within the constraint of fixed gun geometry, modest increases in velocity could be achieved by selecting the appropriate loading parameters to cause shock compression of the light gas.

Throughout the report the criteria for good performance has been implied to be high muzzle velocity. This is not always true in other gun applications. For example, limiting projectile base pressure might be more important than obtaining maximum velocity in order to insure structural integrity of the projectile. The results demonstrate that a significant range of muzzle velocities can be obtained through proper choice of loading parameters. This report adequately describes the performance characteristics of the Texas A&M light-gas gun up to muzzle velocities in the

neighborhood of 18,000 ft/sec. Recommendations are made which could extend the range to even higher muzzle velocities.

One of the first efforts in future work should be to either eliminate or minimize the experimental errors commented on in the preceding section. The powder gas leakage problem could no doubt be reduced through experimentation with various sealing techniques. It has been suggested, for example, that a deformable washer made from a soft material such as lead might improve the powder chamberpump tube seal. In addition, the gas leakage suspected across the piston might be eliminated through experimentation with various more sophisticated piston designs. Figure 17 illustrates a few piston configurations which could be tested.

At present, a plan to install a velocity measurement system which does not rely on physical interruption of the projectile's flight is being carried out. Despite the feeling that the ballistic screen technique used for this study did not introduce serious experimental errors, installation of this new system should entirely eliminate the problem. The technique proposed consists of a laser light source which is used to project light "screens" across the projectile flight path. As the screens are interrupted a high speed counter will record the time of flight over a known distance.

A more basic improvement might be possible through efforts to adjust the nature of the piston-compression process experienced during the launch cycle. As has been mentioned in various sections

NOTE: ALL DIMENSIONS ARE IN INCHES.

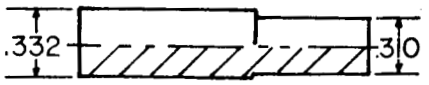

(a) Conventional

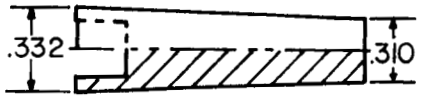

(b) Taper, Expandable Base

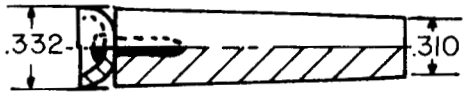

(c) Taper, Washer Seal

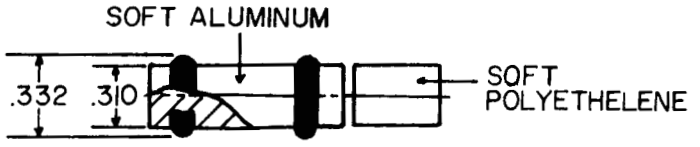

(d) Two Piece, O-Ring Seal

Figure 17 Proposed Piston Designs

of this report, this process can be characterized as either an isentropic compression or a shock compression. The results of this report suggest that the gun is not operating efficiently as either an isentropic or shock compressor. Increasing the average piston velocity would result in higher reservoir pressures and temperatures due to shock compression. To increase the performance of an isentropic compression cycle, a larger compression ratio would be required. This implies a longer pump tube which, under the constraint of working with existing gun components, cannot be obtained. Efforts to operate the existing configuration as a shock compressor is felt to deserve future work. Raising the burst strength of the powder chamber diaphragm is one obvious way in which this could be accomplished.

REFERENCES

1 Seigel, A. E., "The Theory of High Speed Guns," Agardograph 91, May 1965, NATO Advisory Group for Aerospace Research and Development.

2 Berggren, R. E. and Reynolds, R. M., "The Light-Gas Gun Model Launcher," Ballistic-Range Technology, Agardograph 183, August 1970, Chapter 2, pp. 9-56.

3 Glass, I. I., "Hypervelocity Launchers, Part 2: Compound Launcher-Driving Techniques," UTIAS No. 26, Dec. 1965, Institute for Aerospace Studies, University of Toronto.

4 Charters, A. C., Denardo, B. P., and Rossow, V. J., "Development of a Piston-Compressor Type Light-Gas Gun for the Launching of Free-Flight Models at High Velocity," NACA TN 4143, Nov. 1957, Ames Aeronautical Laboratory, Moffett Field, Calif.

5 Baer, P. G. and Smith, H. C., "Interior Ballistics of Hypervelocity Projectors Instrumented Light-Gas Gun and Traveling Charge Gun," Proceedings of the Fifth Symposium on Hypervelocity Impact, USA, UASF, and USN, Vol. 1, Part 1, April 1962, pp. 53-77.

6 Baer, P. G. and Smith, H. C., "Experimental and Theoretical Studies on the Interior Ballistics of Light-Gas Guns," Proceedings of the Sixth Symposium on Hypervelocity Impact, USA, USAF, and USN, Vol. 1, August 1963, pp. 41-105.

7 Piacesi, R., Gates, D. F., and Seigel, A. E., "A Computer Analysis of Two-Stage Hypervelocity Model Launchers," NOLTR 62-87, Feb. 1963, N.O.L., White Oak, Maryland.

8 Collins, D. J., Charters, A. C., Christman, D. R., Sangster, D. K., "Parametric Studies of Light-Gas Guns," Proceedings of the Fifth Hypervelocity Techniques Symposium, University of Denver, Vol. 2, March 1967, pp. 1-34.

9 Porter, C. D., Swift, H. F., and Fuller, R. H., "Summary of NRL Hypervelocity Accelerator Development," Proceedings of the Fifth Symposium on Hypervelocity Impact, USA, USAF, and USN, Vol. 1, Part 1, April 1962, pp. 23-52.

10 Stephenson, W. B. and Anderson, D.E., "Two-Stage Light-Gas Model Launchers," Aerospace Engineering, Vol. 21, No. 8, August 1962, pp. 64-65.

11 Heiney, O. K., "Simplified Interior Ballistics of Propellant-Actuated Devices," SPS 37-43, Vol. IV, Feb. 1967, J.P.L., Pasadena, Calif., pp. 167-170.

12 Heiney, O. K., "Pressure and Density Gradients in Propellant Gases," SPS 37-44, Vol. IV, April 1967, J.P.L., Pasadena, Calif., pp. 87-91.

13 Sutton, G. P., Rocket Propulsion Elements, 3rd ed., Wiley, New York, 1967, pp. 336-337.

14 Baker, J. R., "Light-Gas Gun Performance: Theoretical Analysis and Experimental Comparison," Proceedings of the Seventh Hypervelocity Impact Symposium, USA, USAF, and USN, Vol. 1, Feb. 1965, pp. 23-44.

APPENDIX A

THE TEXAS A&M UNIVERSITY LIGHT-GAS GUN FACILITY

The Texas A&M University (TAMU) light-gas gun was built by NASA-MSC in 1967 as a small portable system for both simulation experiments and demonstrations. At the time of its inception, projectile velocities of 10 Km/sec were anticipated; but initial test shots indicated the performance to be significantly less than expected. As a result the gun was never utilized by NASA-MSC for the wide range of tests originally planned.

The gun along with supporting equipment was loaned to Texas A&M University by NASA-MSC for use under NASA Grant NGR 44-001-106. Installation of the gun was completed in January 1972, at the Texas Engineering Experiment Station (TEES) Hypervelocity Laboratory. Principal investigator for gun research and director of the Hypervelocity Laboratory is Dr. James L. Rand, Associate Professor of Aerospace Engineering.

The gun facility may be conveniently divided into three subsystems: the gun system, the control system, and the instrumentation system, as shown in Figures A-1 and A-2. The first includes the physical components of the gun and flight range as well as the components used for gun mounting and alignment. The control system includes the gas supplies, pressure regulators, and electrical circuits contained in the control console; while the instrumentation

system includes the oscilloscopes, ballistic screens, pressure gauges, and various other equipment used to acquire data.

The gun consists of six primary parts, as shown in Figure A-1. These are (1) the firing magazine, (2) the powder chamber, (3) the pump tube, (4) the high pressure section, (5) the launch tube, and (6) the flight range. The firing magazine, which is internally threaded so that it may be screwed onto the end of the powder chamber, consists of an electronically triggered plunger-type solenoid which strikes the firing pin. The cylindrical stainless steel powder chamber has a removable .458 magnum cartridge holder followed by a nozzle which converges to the pump tube diameter. Following the powder chamber is an 18 inch long pump tube which has a slightly tapered bore beginning at 0.332 in. at the powder chamber junction and decreases to 0.310 in. at the high pressure section entrance. Midway along this pump tube is a small feedhole for the transfer of gases between the control console and the pump tube. Both ends of the pump tube are sealed with o-rings during gun assembly.

The high pressure section which provides a smooth transition from the pump tube bore down to the launch tube bore, is bolted between the pump tube and the launch tube through the use of two large collars. The high pressure sections's bore diameter begins equal to that of the pump tube, which continues for 2 inches, and then enters a 1/2 inch, smoothly contoured nozzle (sometimes referred to as an "aerodynamic" nozzle) which converges to the launch tube bore size. A 1 1/2 in. bore section connects the nozzle with the high pressure

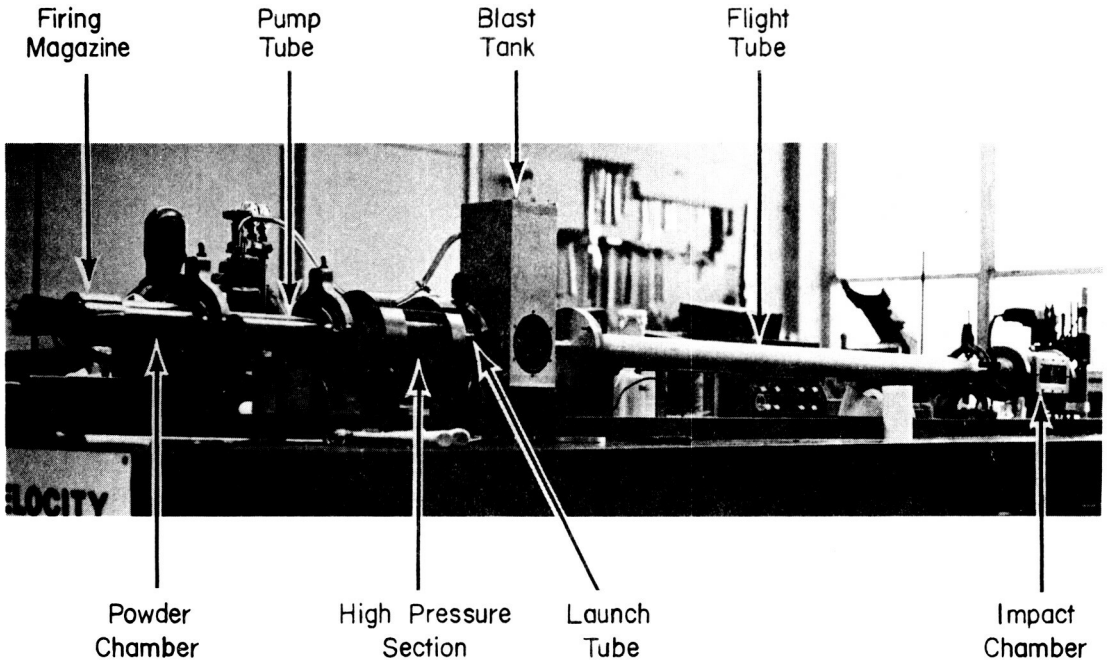

Figure A-1: The Gun System

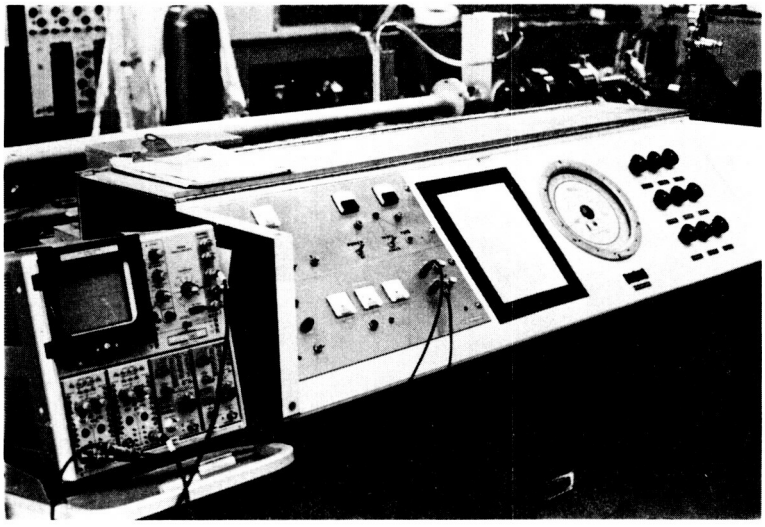

Figure A-2: Gun Instrumentation and the Control Console

section launch tube junction. Both ends are o-ring sealed, and the launch tube end is used to seat the metal diaphragm which controls the projectile release pressure. These diaphragms are nominally 0.005-0.006 in. steel or stainless steel. The launch tube is 9 inches long, and also has a slightly tapered bore which exits into the flight range with a 0.078 in. diameter. The flight range includes a blast tank, a 6 foot flight tube and an impact chamber. The blast tank provides a large volume into which the high pressure gas trailing the projectile may expand. On either side are two portholes which may be covered with either glass windows or aluminum bulkheads. A pressure tap through one wall of the blast tank permits evacuation of the range before firing the gun. The flight tube, which permits separation of a sabot-projectile combination, leads to the impact chamber which has an observation port on either side. The chamber end plate has four threaded studs which provide support for gun instrumentation and the specimen to be impacted. In addition the end plate has four, pressure-sealed, electrical feed through terminals. The chamber has an inside diameter of 4 1/4 inches and an 11 1/2 inch length. Figure A-3 supplies the critical gun dimensions.

The gun control system is consolidated within the confines of a portable control console. Three Linde type R gas containers, which are mounted along the back wall of the console, store the hydrogen, nitrogen, and helium used during normal gun operations. A piping network enables the transfer of gases to either the pump tube or

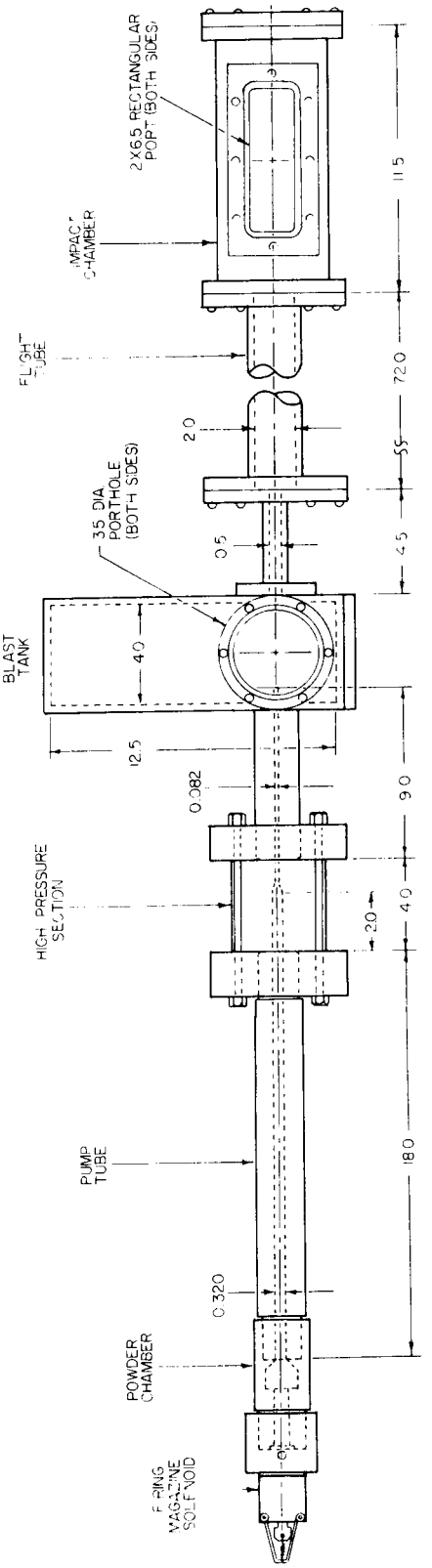

Figure A-3 Gun Dimensions

range or allows venting to the atmosphere. Figure A-4 depicts the network of piping valves and gauges used for controlling the gas flow. A Welch 1/3 horsepower, model 1400, mechanical vacuum pump is part of the system which permits evacuation of the flight range and pump tube. Figure A-5 illustrates the nominal performance of the pump during evacuation of the flight range. A high vacuum McLeod guage, which can sense pressures and be read from 150 torr to 0.001 torr, has been used to monitor flight range pressures to as low as 0.2 torr (200 microns).

Electrical control of the gun is exercised through the circuit shown in Figure A-6. A "fire control" circuit, located in the middle of the figure, prevents triggering of the firing solenoid until a safety switch is opened. When the gun is fired a capacitor bank is allowed to discharge into the solenoid. This provides an additional safety feature in that the gun cannot be re-fired until the safety switch is closed which allows the capacitor to re-charge.

Gun instrumentation has been primarily used to obtain accurate projectile velocity measurements thus far. The system utilized employs two ballistic screens, positioned a known distance apart, along the anticipated flight path of the projectile. Each screen consists of a strip of paper which has a continuous printed circuit on one side. As the projectile pierces the strip, the circuit is broken, thereby providing a signal which may be displayed on an oscilloscope or may be used to start or stop an electronic counter. Future work at the Hypervelocity Laboratory includes the replacement of the

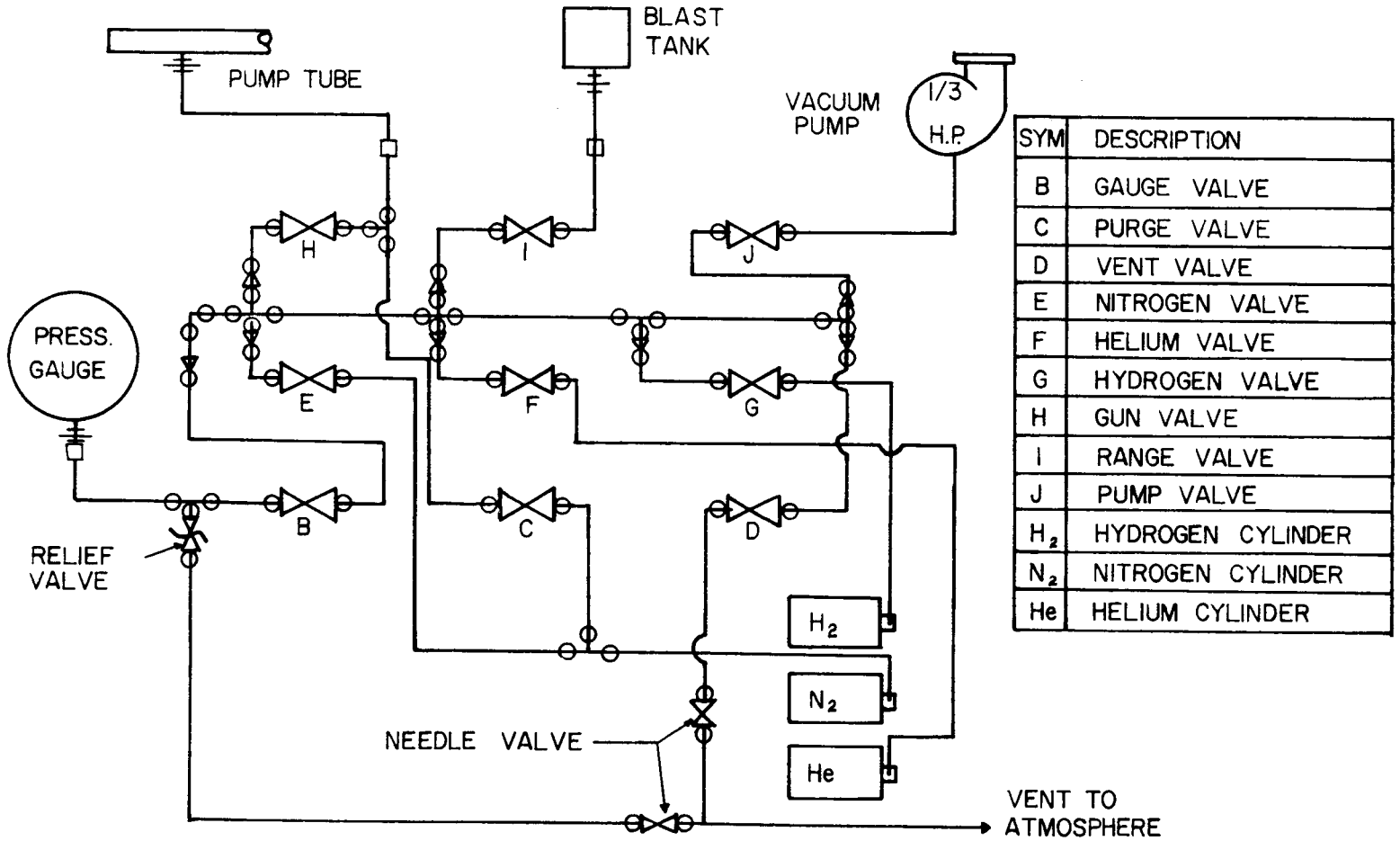

SYM	DESCRIPTION
B	GAUGE VALVE
C	PURGE VALVE
D	VENT VALVE
E	NITROGEN VALVE
F	HELIUM VALVE
G	HYDROGEN VALVE
H	GUN VALVE
I	RANGE VALVE
J	PUMP VALVE
H_2	HYDROGEN CYLINDER
N_2	NITROGEN CYLINDER
He	HELIUM CYLINDER

Figure A-4: Piping Schematic Diagram

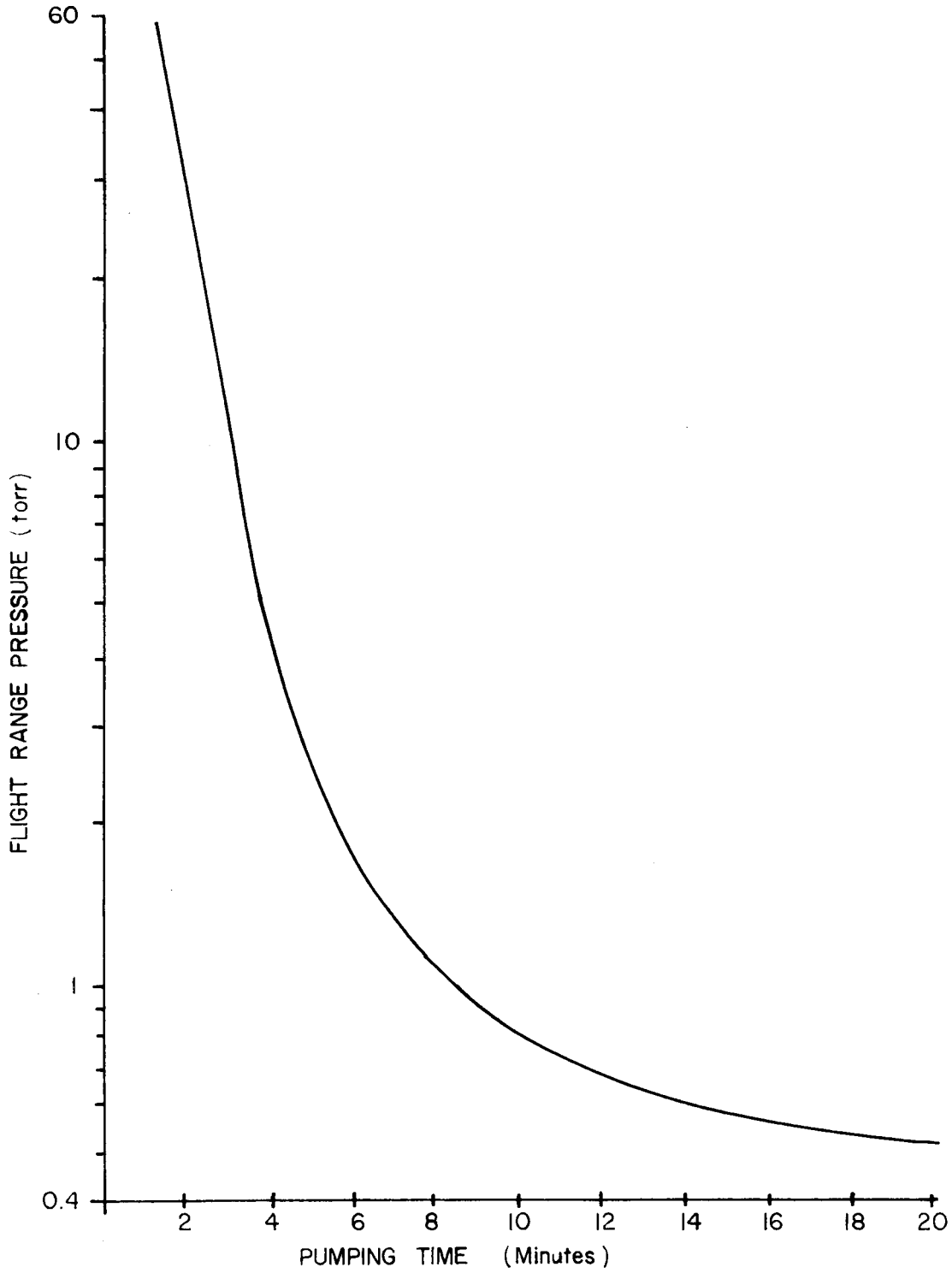

Figure A-5: Typical Pressure-Time Plot for the 1/3 H.P. Welch Vacuum Pump

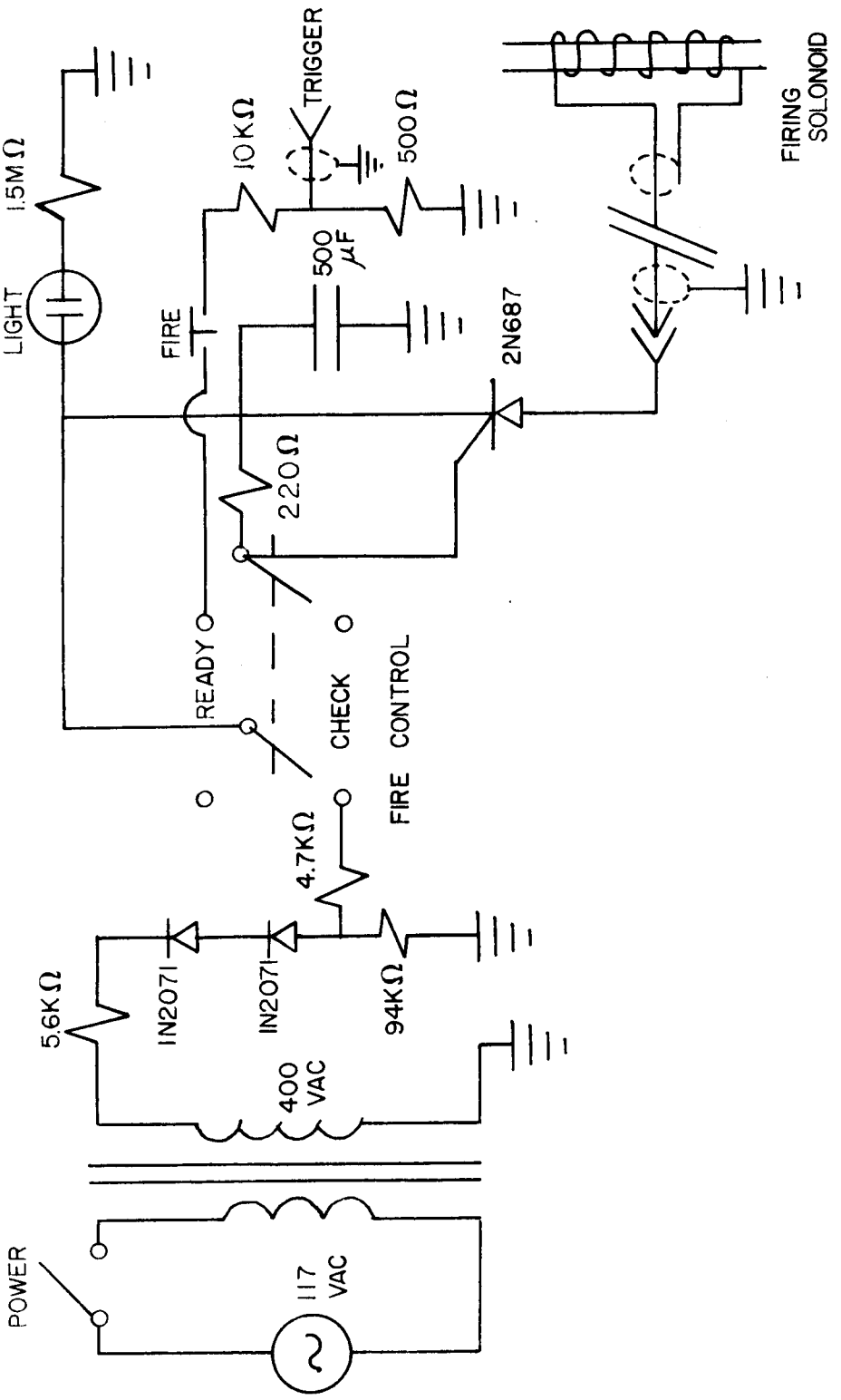

Figure A-6: Light Gas Gun Firing Circuit

ballistic paper screens by "light" screens eminating from a laser light source. The principle is basically the same as with the ballistic paper; however, under the new system, the projectile interrupts a stream of light rather than having to physically impact paper strips. The following equipment is available for gun instrumentation and for support of the facility as a whole:

3-Hewlett-Packard Model 141A Oscilloscopes

1-Tektronix Model 7504 Oscilloscope

3-Hewlett-Packard Model 1402A Dual Trace Amplifiers

2-Hewlett-Packard Model 1420A Time Bases

1-Hewlett-Packard Model 1421A Time Base & Delay Generator

2-Tektronix Model 7A12 Dual Trace Amplifiers

1-Tektronix Model 7B50 Time Base

1-Tektronix Model 7B51 Time Base & Delay Generator

1-Datapluse Model 101A Pulse Generator

1-Beckman Universal EPUT and Timer Model 7360 JR

1-CMC Frequency-Period Counter Model 203A

1-Hewlett Packard Model 5302A Universal Counter

2-Hewlett Parckard Model 461A Wide Band Amplifiers

1-Spectral Physics - 1/2 milliwatt laser

1-Sartorius Model 2401 Laboratory Balance

1-Hewlett Packard Model 197A Oscilloscope Camera

1-Tektronix Model c-12 Oscilloscope Camera

1-6" Lathe with 48" bed

1-Derbyshire Jewelers Lathe

APPENDIX B

EXPERIMENTAL RESULTS

SHOT NO.	DATE	POWDER CHG. TYPE	POWDER CHG. gms	PISTON MASS TYPE	PISTON MASS gms	PUMP TUBE GAS TYPE	PUMP TUBE GAS psia	SHEAR DISK[a] TYPE	SHEAR DISK[a] gms	PROJECTILE TYPE	PROJECTILE gms	VELOCITY ft/sec	REMARKS
1A	6/08/72	RP-2400[b]	2.01	POLY[c]	1.50	H_2	50	S.S.[d]	.001	LEX[e]	.016	11,000	No Scope Picture
2A			2.01		1.49		50		.005		.011	------	Miss on 2nd Ballistic Paper
3A			2.03		1.54		75		.008		.012	------	Miss on 1st Ballistic Paper
4A			2.01		1.48		75		.005		.011	------	No Picture, Projectile broke up
5A	6/09/72		2.01		1.48		75		.007		.014	9,700	Good Shot
6A			2.01		1.47		100		.004		.011	9,100	Good Shot
7A			2.00		1.47		100		.009		.008	9,400	Good Shot
8A			2.01		1.46		75		.004		.017	8,4007	No Clean Hit on 2nd Paper
9A	6/12/72		2.01		1.48		75		.003		.013	11,300	Good Shot
10A			2.01		1.53		50		.007		.014	10,100	Good Shot
11A			2.01		1.45		125		.004		.011	8,500	Good Shot
12A			2.01		1.45		125		.006		.012	9,000	Powder Chamber Leak
13A	6/13/72		2.01		1.50		100		.005		.008	9,300	Good Shot
14A			2.01		1.53		100		----		.010	13,000	Good Shot
14XA			2.00		1.53		100	S.S.	----		.008	12,100	Good Shot
15B	6/14/72	RP-2400	2.00	POLY	1.50	H_2	100	STL[f]	.004	LEX	.010	10,600	No Picture
16B			2.01		1.52		100		.005		.010	12,900	Good Shot
17B	6/15/72		2.01		1.51		100		.005		.009	12,800	Ionization Gauge Test, Good Shot
18B	6/16/72		2.00		1.50		125		.005		.012	11,700	Good Shot
19B	6/19/72		2.01		1.50		75		.007		.011	13,200	Good Shot
20B	6/21/72		2.01		1.51		75		.003		.012	11,500	Powder Chamber Leak
21B	6/22/72		2.01		1.50		75		.005		.011	12,100	Good Shot
22B			2.00		1.51		50		.008		.011	11,900	Good Shot
23B			2.00		1.50		50		.005		.009	9,100	Good Shot
24B	6/28/72		2.00		1.50		125		.004		.010	11,900	Good Shot
25B			2.00		1.50		150		.005		.010	12,500	Good Shot
27C	6/26/72	RP-2400	2.51	POLY	1.50	H_2	50	STL	----	LEX	.009	------	No Picture, Gun Clogged
27XC			2.50		1.51		50		.002		.010	9,200	Good Shot

SHOT NO.	DATE	POWDER CHG. TYPE	POWDER CHG. gms	PISTON MASS TYPE	PISTON MASS gms	PUMP TUBE GAS TYPE	PUMP TUBE GAS psia	SHEAR DISK TYPE	SHEAR DISK gms	PROJECTILE TYPE	PROJECTILE gms	VELOCITY ft/sec	REMARKS
28C	6/26/72	RP-2400	2.50	POLY	1.50	H_2	50	STL	.003	LEX	.014	11,100	Powder Chamber Leak
29C			2.50		1.50		75		----		.011	------	No Picture, Miss on 2nd Paper
29XC			2.50		1.50		75		.004		.011	11,600	Good Shot
30C			2.50		1.50		75		.007		.011	10,800	Good Shot
31C	6/27/72		2.51		1.50		100		.003		.013	12,600	Good Shot
32C			2.50		1.50		100		.005		.017	12,300	Good Shot
33C			2.50		1.50		125		----		.013	------	No Picture, Miss on 2nd Paper
33XC			2.50		1.50		125		.002		.015	12,300	Good Shot
34C			2.50		1.50		125		.005		.012	8,4007	Miss on 2nd Ballistic Paper
34XC			2.50		1.50		125		----		.012	------	Miss on 2nd Ballistic Paper
35C			2.50		1.50		150		.003		.009	14,300	Good Shot
36C			2.50		1.50		150		----		.011	10,600	Powder Chamber Leak
37C	6/28/72		2.51		1.51		150		----		.011	------	Miss on 2nd Ballistic Paper
37XC			2.50		1.51		150		.004		.013	14,600	Good Shot
38C			2.50		1.51		150		.005		.013	15,900	Good Shot
39C	6/29/72		2.51		1.51		137.5		----		.011	------	Miss on 2nd Ballistic Paper
39XC	6/30/72		2.50		1.50		137.5		.005		.016	13,300	Good Shot
40C	6/30/72		2.50		1.50		137.5		.005		.014	13,000	Good Shot
41C			2.50		1.51		162.5		.004		.014	13,600	Good Shot
42C			2.51		1.51		162.5		.005		.013	------	Miss on 2nd Ballistic Paper
43D	7/06/72	RP-2400	2.50	POLY	1.50	H_2	150	S.S.	.003	LEX	.015	13,600	Good Shot
44D			2.50		1.49		150		.006		.014	13,300	Good Shot
45D			2.51		1.49		125		.004		.012	14,000	Good Shot
46D			2.50		1.48		125		.009		.014	11,800	Powder Chamber Leak
47D			2.50		1.51		100		.005		.015	15,200	Good Shot
48D	7/07/72		2.50		1.50		100		.005		.008	14,600	Good Shot
49D			2.51		1.50		75		.004		.010	15,200	Good Shot
50D			2.50		1.50		75		----		.008	14,000	Good Shot

SHOT NO.	DATE	POWDER CHG. TYPE	POWDER CHG. gms	PISTON MASS TYPE	PISTON MASS gms	PUMP TUBE GAS TYPE	PUMP TUBE GAS psia	SHEAR DISK[a] TYPE	SHEAR DISK gms	PROJECTILE TYPE	PROJECTILE gms	VELOCITY ft/sec	REMARKS
51	7/08/72	RP-2400[b]	2.50	POLY[c]	1.50	H_2	100	2X S.S.[h]	.010	LEX[e]	.010	14,000	Good Shot
52			3.00		1.50		100	S.S.[d]	.004		.012	14,000	Good Shot, Powder Chamber Leak
53	7/10/72		2.50	POLY/LD[g]	5.11		150	STL[f]	.003		.012	15,900	Good Shot
54	7/11/72		2.50		5.13		150		.003		.014	16,200	Poor Scope Picture
55			2.50		5.02		150		.003		.011	17,900	Good Shot
56	7/16/72		2.51		5.05		100		.003		.012	15,900	Good Shot
57			2.50		4.73		125		.003		.011	16,600	Good Shot
58			3.00		5.03		150		.004		.013	17,900	Good Shot, Powder Chamber Leak
59			3.00		5.08		150		.004		.012	19,000	Good Shot, Powder Chamber Leak
60	7/17/72		3.50		3.98		150	S.S.	.005		.010	18,100	Good Shot, Powder Chamber Leak
61	7/18/72		3.50		4.50		150	2X S.S.	.008		.010	17,900	Tapered Piston, Good Shot
62	7/19/72		3.00		4.89		150	2X S.S.	.008		.008	16,700	Powder Chamber Leak

a Shear Disk - refers to that portion of the burst diaphragm which is accelerated with the projectile.

b RP-2400 - Abbreviation identifying gunpowder propellant used. Refers to type 2400 smokeless rifle powder.

c POLY - Abbreviation for high density (Type F) polyethelene.

d S.S. - .005 inch thick, Stainless Steel. Burst pressure is 20,000 psi (Ave).

e LEX - Abbreviation for "Lexan" plastic (Commercially available trade name).

f STL - .006 inch thick, Steel. Burst pressure is 12,000 psi (Ave).

g POLY/LD - Piston with lead weight added.

h 2X S.S. - Two Stainless Steel diaphragms inserted behind projectile. Burst pressure is 32,000 psi (Ave).

APPENDIX C

O. K. CODE NOMENCLATURE AND PRINTOUT

PROGRAM NOMENCLATURE

ACEL = Acceleration of the piston

ALEA = Cross-sectional area of barrel

ALGT = Acceleration of the projectile

AREA = Cross-sectional area of pump tube

BARE = Burning area of propellant (propellant types 1,2,4,5)

BARI = Burning area of propellant (propellant type 3)

BDIS = Piston travel

BETA = Heat loss coefficient for powder gas

BLIS = Projectile travel

BLTA = Heat loss coefficient for light gas

BP = Mass of propellant burned

CHG = Initial powder charge weight

CPEG = Projectile base pressure

CPIC = Projectile muzzle velocity

CPLG = Average light gas pressure

CPRS = Average powder gas pressure

CVL = Covolume (η) for light gas

CVOL = Powder chamber volume

DAN = Diameter for ball type propellant

DELTA = Time increment

DFLG = "δ" factor for light gas

DIN = Propellant grain inside diameter

DLDT = Piston velocity

DOT = Propellant grain outside diameter

DPDT = Pressure slope in powder gas

DPLG = Pressure slope in light gas

DTDT = Temperature slope in light gas

EFM = Effective or psuedo mass

FIMP = Impetus of powder propellant

FPU = Fraction of propellant burned

FVOL = "Free" volume of powder gas

GAMA = Specific heat ratio of powder gas

GIN = Initial powder gas density

GMLG = Specific heat ratio of light gas

GN = Powder gas density

GRNS = Number of propellant grains

HCPP = Peak pressure in powder gas

HGBL = Barrel length

HGID = Initial light gas density

HGIP = Initial light gas pressure

HGIT = Initial light gas temperature

HGIV = Initial light gas volume

HGM = Mass of light gas

HGSM = Weight of projectile

HLGP = Light gas peak pressure

IPT = Identifies propellant type

PIT = 1.5, empirical correction factor

PFAC = "S" factor for powder gas

PLGR = Isentropic pressure ratio in light gas

PREX = Piston base pressure

PRS = Array of powder chamber pressures

PSL = δ array for light gas

PSY = δ array for powder gas

RFST = Diaphragm burst pressure or projectile release pressure

RHO = Propellant weight density

RTF = Universal gas constant (Units = ft - $lb_f/lb_{mole}{}^{o}K$)

RUN = Pump tube length

SABPR = Powder diaphragm burst pressure or piston release pressure

SCPRS = Initial powder chamber pressure

SHOT = Piston mass

TIME = Elapsed time

TF = Flame temperature of propellant

TLGS = Average light gas temperature

TYPE = Output array to write propellant name

UBW = Unburned propellant volume

VEE = Velocity array for powder gas

VEL1 = Old piston velocity

VEL2 = New piston velocity

VLE = Velocity array for light gas

VLG = Projectile velocity

VLGS = Light gas volume

WEB = Propellant grain thickness

WMAL = Light gas molecular weight

WMOL = Powder gas molecular weight

XLIN = Length of propellant grain

```
      IMPLICIT REAL *8(A-H,O-Z)
      DIMENSION PSY(30), VEE(30)
      DIMENSION PRS(40), RATE(40), TYPE(8)
      DIMENSION PROPF(4,3)
      DIMENSION FMT(18), FMT1(4), FMT2(13), DATA(4)
      DIMENSION PSL(30), VLE(30)
      COMMON/   /PCPRS(1000), PBDIS(1000), RUN, PTOP, NPTS
      COMMON/PLTHDR/ SHOT, CHG, WEB, CVOL, AREA, VM
      READ(5,3)FIMP, GAMA, RHO, CVL, (TYPE(N),N=1,4)
    3 FORMAT(F8.1,F8.3,F8.4,F8.2,4A2)
      READ(5,7) AREA,CVOL,RUN,WEB,BETA,SCPRS,SABPR
    7 FORMAT(2F7.3,F7.1,F7.4,F7.2,2F8.1)
      READ(5,14) HGBL,HGIV,HGIT,ALEA,BLTA
   14 FORMAT(5F10.0)
      READ(5,110) IPT,DAN,DOT,DIN,XLIN,WMOL
  110 FORMAT(I1,5F10.7)
C     ************************************************************************
      PRS(1)=50.0
      RATE(1)=0.134
      AN=0.5
      B=0.0189
      DO 5 I=1,39
      PRS(I+1)=1000.*I
      RATE(I+1)=B*(PRS(I+1)**AN)
    5 CONTINUE
C     ************************************************************************
      VLE(1)=0.0
      PSL(1)=3.0
      AN=2.195
      B=(.00793/1000000.)
      DO 24 I=1,29
      VLE(I+1)=1000.*I
      PSL(I+1)=3.0+B*(VLE(I+1)**AN)
   24 CONTINUE
C     ************************************************************************
```

```
      VEE(1)=0.0
      PSY(1)=3.0
      AN=2.263
      B=(.00294/1000000.)
      DO 26 I=1,29
      VEE(I+1)=1000.*I
      PSY(I+1)=3.0+B*(VEE(I+1)**AN)
   26 CONTINUE
C     ********************************************************************************
      PIT=1.5
      TAD=GAMA/(GAMA-1.)
    6 READ(5,41) SHOTU,CHGU,HGIP,RFST,HGSMU
   41 FORMAT(5F10.2)
      IF(IPT.LT.1.OR.IPT.GT.5) IPT=1
   16 NPTS=0
      XLGS=HGIV
      SHOT=SHOTU*o.0022
      CHG=CHGU*0.0022
      HGSM=HGSMU*0.0022
      EFM=0.0
      ACEL=0.0
      VEL1=0.0
      AVOL=CVOL
      R=0.0
      RAT=0.0
      NPTS=0
      BLIS=0.0
      HLGP=0.0
      KEY=0
      HCPP=0.0
      ILF=1
      JFG=0
      RTF=2780.
      KUE=-1
      VLG=0.0
```

```
      ALGT=0.0
      TLGS=HGIT
      DTDT=0.0
      GMLG=1.41
      GLG=GMLG-1.
      WMAL=2.0
      DPLG=0.0
      GAG=1.-(1./GMLG)
      CPLG=HGIP
      CPEG=CPLG
      TIME=0.0
      DELTA=0.0001
      VLGS=HGIV
      HGID=HGIP*WMAL/(RTF*HGIT*12.)
      HGM=HGID*HGIV
      BP=0.0
      VEL=0.0
      IF(WMOL.LE.0.0) WMOL=24.
      TF=WMOL*FIMP/RTF
      XTF=TF
      GIN=SCPRS*WMOL/(RTF*TF*12.)
      FVOL=CVOL-(CHG/RHO)
      GO TO (125,123,120,123,123),IPT
  120 FPU=0.0
      RT=0.0
      BARI=5.*CHG/(RHO*WEB)
      GO TO 130
  123 AOT=DOT*DOT*3.1417/4.
      AIN=DIN*DIN*3.1417/4.
      IF(IPT.EQ.4) AIN=7.0*AIN
      IF(IPT.EQ.5) AIN=19.0*AIN
      AEF=AOT-AIN
      GRNS=CHG/(AEF*XLIN*RHO)
      GO TO 130
  125 BARE=2.*CHG/(RHO*WEB)
```

```
130 WRITE(6,146)
146 FORMAT(1H1,44(1H$),'  DATA FOR THE TEXAS A&M LIGHT GAS GUN  ', 44(
   11H$))
    WRITE(6,8)
  8 FORMAT(1HO,61H  PSTN WT.   CHARGE     WEB   B.LENGTH   CHB VOL
   1BORE AREA//)
    WRITE(6,9)SHOTU,CHGU,WEB,RUN,CVOL,AREA
  9 FORMAT(F10.2,F10.3,F10.4,F10.1,F10.2,F10.2///)
    WRITE(6,29)
 29 FORMAT(24H   LIGHT GAS GUN DATA   ,60H   PROJ WEIGHT   B.LENGTH
   1CHB VOL.   BORE AREA   HEAT LOSS)
    WRITE(6,25) HGSMU,HGBL,HGIV,ALEA,BLTA
 25 FORMAT(27X,F11.5,F11.2,F11.2,F12.3,F12.2
    DATA(1)=WMOL
    DATA(2)=XLIN
    DATA(3)=DOT
    DATA(4)=DIN
    WRITE(6,30)WMOL,BETA,(TYPE(N),N=1,4)
 30 FORMAT(//21H  MOLECULAR WEIGHT = ,F5.1,23H   HEAT LOSS FACTOR IS ,
   1F5.2,32H   PROPELLANT USED IN SYSTEM IS ,4A2//)
    GO TO (31,33,35,37,61),IPT
 31 WRITE(6,32)
 32 FORMAT(58H   PROPELLANT FORM IS SINGLE PERFORATE OR CONSTANT SURFA
   1CE//)
    GO TO 60
 33 WRITE(6,34)
 34 FORMAT(47H   PROPELLANT FORM IS DETERRED SINGLE PERFORATE//)
    GO TO 60
 35 WRITE(6,36)
 36 FORMAT(35H   PROPELLANT FORM IS DETERRED BALL//)
    GO TO 60
 37 WRITE(6,38)
 38 FORMAT(47H   PROPELLANT FORM IS DETERRED SEVEN PERFORATE//)
    GO TO 60
 61 WRITE(6,62)
```

```
   62 FORMAT(49H   PROPELLANT FORM IS DETERRED NINETEEN PERFORATE//)
   60 WRITE(6,95)
   95 FORMAT(2X,11H**********,10X,18H   PROPELLANT SIDE, 10X,13H********
     1*****,5X,13H*************,10X,14HLIGHT GAS SIDE, 10X,10H**********)
      WRITE(6,96)
   96 FORMAT(8X,4HTIME,4X,10HCHAMB PRES, 4X,6HTRAVEL,4X,11HPROP BURN    ,10
     1HPRES SLOPE,3X,17HVELOCITY**CB PRES,3X,8HVELOCITY,6X,6HTRAVEL,3X,7
     2HBS PRES,6X,4HTEMP
      BP = 0.0
      VEL2=0.0
      BDIS=0.0
      PTOP=3000.
      CPRS=SCPRS
      GAMB=(1.+BETA)*(GAMA-1.)
      DO 39 J=1,3000,1
      IF(BLIS.GE.HGBL) GO TO 79
      GO TO (74,135,74,134,134),IPT
  134 IF (RAT-WEB) 135,74,74
  135 RAT=R*.00005
      DIN=DIN+RAT
      XLIN=XLIN-RAT
      AIN=DIN*DIN*3.1417/4.
      AIX=DIN*3.1417
      IF(IPT.NE.4) GO TO 132
      AIN=7.0*AIN
      AIX=7.0*AIN
      GO TO 136
  132 IF(IPT.NE.5) GO TO 136
      AIN=19.0*AIN
      AIX=19.0*AIN
  136 AEF=AOT-AIN
      BARE=GRNS*(2.*AEF+XLIN*AIX)
   74 JA=1
      IF(CPRS.LT.300.0) GO TO 76
   78 IF(CPRS-PRS(JA)) 77,76,75
```

```
 75  JA=JA+1
     GO TO 78
 76  R=RATE(JA)
     GO TO 10
 77  DIT=PRS(JA)-PRS(JA-1)
     DAT=RATE(JA)-RATE(JA-1)
     PIG=CPRS-PRS(JA-1)
     DIM-((PIG/DIT)*DAT)
     R=RATE(JA-1)+DIM
 10  KG=1
     IF(VLG.LT.VLE(1)) GO TO 93
  91 IF(VLG .GT. VLE(#))) GO TO 115
     IF(VLE(KG)-VLG) 92,92,94
 92  KG=KG+1
     GO TO 91
 93  DFLG=PSL(KG)
     GO TO 90
 94  HIG=(VLG-VLE(KG-1))/(VLE(KG)-VLE(KG-1))
     DFLG=(PSL(KG)-PSL(KG-1))*HIG+PSL(KG-1)
 90  PHGM=HGM/(DFLG*32.174)
     IF (BP-CHG)11, 80,80
 80  DNDT=0.
     GO TO 12
 11  IF (IPT.NE.3) GO TO 140
     IF(RT-DAN) 145,145,150
145  R=(R/1.6)*(1.+(.6*RT/DAN))
     RT=RT+R*DELTA
150  (IF(FPU-.9) 155,155,140
155  BARE=BARI*(1.-(FPU**1.7))
140  DNDT=R*RHO*BARE
     BP=BP+(DNDT*DELTA)
     IF(HCPP.LT.CPRS) HCPP=CPRS
     IF(JFG.GT.1) GO TO 12
     IF(CPRS.LT.SABPR) GO TO 54
     DELTA=.000010
```

```
   19  ILF=5
   20  ALGT=CPEG*32.17*ALEA/HGSM
       VLGI=VLG
       VLG=VLGI+(ALGT*DELTA)
       BLIC=(VLGI*DELTA)+(ALGT*DELTA*DELTA/2.)
       BLIS=BLIS1+BLIC*12.
    23 TLGS=TLGS1+DTDT*DELTA
       IF(TLGS . LT. 0.0) GO TO 1004
       GO TO 1005
  1004 DELTA=0.5*DELTA
       NO=NO+1
       IF (NO . GT. 100) GO TO 117
       GO TO 101
  1005 CONTINUE
C      ********************************************************************************
       SPEED=DSQRT(GMLG*RTF/WMAL*TLGS)
C      ********************************************************************************
   18  DLDT=VEL2
       XLGS=HGIV+(BLIS*ALEA)-(BDIS*AREA)
       CHUCK=XLGS/AREA/(VEL2+SPEED)
       IF(KEY .GT. 0) GO TO 777
       IF(ILF-3) 666,666,555
   555 CHOCK=0.10*DSQRT(ALEA)/(VLG+SPEED)
       IF(CHUCK .LT. 0.0) CHUCK=CHOCK)
       IF(CHOCK .LT. CHUCK) CHUCK=CHOCK
       KEY=1
       GO TO 100
   666 CONTINUE
       IF(CHUCK .LT. 0.0) DELTA=.5*DELTA
       IF(CHUCK .LT. 0.0) GO TO 101
       IF(DELTA .GT. CHUCK) GO TO 100
   777 KEY=0
       GLEX=-GMLG/GLG
       PLGB=1.+(GLG*VLG*VLG*WMAL/(64.3*TLGS*RTF*GMLG))
       IF(PLGB .LT. 0.0) GO TO 143
```

```
444 PLGR=PLGB**GLEX
    CPEG=CPLG*PLGR
    IF(CPEG .LT. 0.0) GO TO 141
    VLGS=XLGS-CVL*HGM/3.
    IF (DFLG.EQ.0.) PHGM=0.
    IF (DFLG.EQ.0.) GO TO 28
    PHGM-HGM/(DFLG*32.17)
28  CONTINUE
    PLGA=12.*CPLG*AREA*VEL2/VLGS
    EFGL=(PHGM+(HGSM/32.17))*(BLTA+1.)
    PLGB=12.*CPGL*ALEA*VLG/VLGS
    PLGC=12.*EFGL*VLG*ALGT*GLG/VLGS
    PLGD=12.*HGM*RTF*DTDT/(VLGS*WMAL)
    DPLG=PLGA-PLGB-PLGC+PLGD
    DTDT=TLGS*DPLG*GAG/CPLG
    IF (ILF-3) 54,54,56
54  KUE=KUE+1
    IF (KUE.EQ.4) GO TO 65
    GO TO 57
65  KUE=0
56  CONTINUE
    WRITE(6,99) TIME, CPRS, BDIS, FPU, DPDT, DLDT, CPLG, VLG, BLIS, CPEG, TLGS
99  FORMAT (F12.7,F12.1,F12.3,F12.4,F14.2,F8.2,5F11.2)
57  CONTINUE
    IF (HLGP.LT.CPLG) HLGP=CPLG
    CPLG=CPLG+(DPLG*DELTA)
    DLDT=VEL2
    UBW+(CHG-BP)/RHO
    COVL=CVL*BP
    DPDT=((DNDT*FIMP*12.)-((GAMB*EFM*ACEL*VEL2*12.)+(AREA*CPRS*VEL1*12
   1.)))/(AVOL-(UBW+COVL))
    DOPE=J
    TIME=TIME+DELTA
    FPU=BP/CHG
    IF (CPRS.GT.PTOP) PTOP=CPRS
```

```
      GN=(GIN*FVOL+BP)/(AVOL-(UBW + COVL))
      TF=CPRS*WMOL/(GN*RTF*12.)
      CPRS=CPRS+(DPDT*DELTA)
   39 CONTINUE
   79 CONTINUE
      CNIT=(BLIS-HGBL)/HGBL
      CPIC-(VLG-VLGI)*CNIT_VLG
      WRITE(6,111) CPIC
  111 FORMAT(///10X,33H LIGHT GAS GUN MUZZLE VELOCITY IS,F8.1,6HFT/SEC)
      WRITE(6,112) HLGP
  112 FORMAT(10X,26HLIGHT GAS PEAK PRESSURE IS,F8.1,4H PSI)
      WRITE(6,113) HCPP
  113 FORMAT(10X,32HCOMBUSTION SIDE PEAK PRESSURE IS, F8.1,4H PSI,////)
      GO TO 119
  115 WRITE(6,116)
  116 FORMAT(1HO,10X,'VELY OR VLG IS TOO BIG ')
      GO TO 119
  117 WRITE(6,118)
  118 FORMAT(1HO,10X,' I AM STUCK IN A TEMP-TIME LOOP ')
      GO TO 119
  141 WRITE(6,142)
  142 FORMAT(1HO,10X,' FURTHER COMPUTATION WOULD BE FRIVOLOUS ')
      GO TO 119
  143 WRITE(6,144)
  144 FORMAT(1HO,10X,' IMPENDING DOOM ')
  119 CONTINUE
      GO TO 6
      END
```